Broadcast Approach to Multiple Access With Local CSIT

Maha Zohdy, *Student Member, IEEE*, Ali Tajer, *Senior Member, IEEE*, and Shlomo Shamai (Shitz), *Life Fellow, IEEE*

***Abstract*— A two-user multiple access channel is considered, in which the channels undergo slow block fading and the state of each channel is known only to its corresponding transmitter. This paper proposes a novel broadcast strategy for multiple access communication in this channel. In the broadcast approach, in principle, a transmitter with CSI uncertainty sends multiple independent superimposed information layers where the rate of each layer is adapted to a specific channel realization. In the existing broadcast approaches to multiuser communication, the transmitters often directly adopt a single-user strategy and each transmitter adapts its transmission to one unknown channel. The novel aspect of the proposed strategy is that it adapts the designed codebooks to the state of the entire network. This is motivated by the fact that the contribution of each user to the network-wide measures (e.g., capacity region) depends not only on the user's direct channel to the receiver, but also on the qualities of other channels. Average achievable rate region and outer bounds on the capacity region are characterized. Furthermore, the *expected* capacity region is investigated, where most part of the capacity region boundary is characterized. Finally, an asymptotic capacity region is also characterized.**

***Index Terms*— Broadcast, local CSIT, MAC, slow fading.**

I. Introduction

WIRELESS channels are often subject to random variations resulting from the surrounding environment, inducing uncertainties about the channel state at all transmitters and receivers in the network. While receivers can estimate the varying channel states with high fidelity, acquiring such estimates at the transmitters via feedback from the receivers incurs additional communication and delay costs. In certain systems, it is not always feasible for the transmitters to acquire the channel state information (CSI) due to, e.g., stringent delay constraints or excessive feedback costs. Under such assumptions, the notion of outage analysis is useful for assessing the reliability of wireless networks [1] and [2]. The outage and delay-limited capacities are studied extensively for various channel models (c.f. [3]–[8] and references therein).

An effective approach to circumvent uncertainty about CSI at the transmitters (CSIT) is a form of superposition coding according to which each transmitter splits its data stream into a number of independently-generated coded layers with different rates. The rate of each layer is adapted to a specific channel state. The transmitter then superimposes and transmits all the generated layers and the receiver decodes as many layers as the actual quality of the channel affords. The broadcast strategy was initially motivated by the superposition coding designed for compound broadcast channels [9]. Based on that, a broadcast strategy was first introduced in [10] for the Gaussian slowly-fading single-user channel in which the transmitter sends an infinite number of superimposed coded information layers each adapted to a different channel state, thus creating an equivalent broadcast network. In such network each channel state can be treated as a different receiver, and it is considered to be degraded with respect to a subset of the remaining states. Hence, each receiver is able to decode its intended information layer in addition to those adapted to all the channels with degraded states. An information-theoretic framework for the notion of variable-to-fixed channel capacity without feedback is studied in [11]. Further, multiple-layer variable-rate systems under the assumption of quantized feedback are investigated in [12].

The information-theoretic limits of the multiple access channel (MAC) when all the transmitters and receivers have *complete* CSI are well-investigated in [1], [13], and [14]. Furthermore, there exists rich literature on the information-theoretic limits of the MAC under varying degrees of availability of *instantaneous* CSIT. Representative studies on the capacity region include the impact of degraded CSIT [15], quantized and asymmetric CSIT [16], asymmetric delayed CSIT [17], non-causal asymmetric partial CSIT [18], and symmetric noisy CSIT [19]. Bounds on the capacity region of the memoryless MAC in which the CSIT is made available to a different encoder in a causal manner are characterized in [20]. Counterpart results are characterized for the case of common CSI at all transmitters in [21], which are also extended in [22] to address the case in which the encoder compresses previously transmitted symbols and the previous states. Studies in [23] provides an inner bound on the capacity region of the discrete and Gaussian memoryless two-user MAC in which the CSI is made available non-causally to one of the encoders.

Manuscript received November 7, 2018; revised April 21, 2019 and July 10, 2019; accepted July 24, 2019. Date of publication August 6, 2019; date of current version November 19, 2019. The work of M. Zohdy and A. Tajer was supported in part by the U.S. National Science Foundation CAREER Award 1554482, and the Thomas Jefferson Fund. The work of S. Shamai has been supported by the European Union's Horizon 2020 Research And Innovation Programme, grant agreement no. 694630. The associate editor coordinating the review of this article and approving it for publication was V. Stankovic. *(Corresponding author: Ali Tajer.)*

M. Zohdy and A. Tajer are with the Department of Electrical, Computer, and Systems Engineering, Rensselaer Polytechnic Institute, Troy, NY 12180 USA (e-mail: tajer@ecse.rpi.edu).

S. Shamai is with the Department of Electrical Engineering, Technion Israel Institute of Technology, Haifa 3200003, Israel.

Color versions of one or more of the figures in this article are available online at http://ieeexplore.ieee.org.

Digital Object Identifier 10.1109/TCOMM.2019.2933515

An inner bound on the capacity of the Gaussian MAC is derived in [24] when both encoders are aware of the CSI in a strictly causal manner. The capacity region of a cooperative MAC with partial CSIT is characterized in [25]. The capacity region of the multi-user Gaussian MAC in which each interference state is known to only one transmitter is characterized within a constant gap in [26]. A two-user generalized MAC with correlated states and non-causally known CSIT is studied in [27]. In [28] a two-user Gaussian double-dirty compound MAC with partial CSIT is studied. The capacity regions of a MAC with full and distributed CSIT are analyzed in [29]. A two-user cooperative MAC with correlated states and partial CSIT is analyzed in [30]. The study in [31] characterizes inner and upper bounds on the capacity region of a finite-state MAC with feedback.

However, when the transmitters can only acquire the probability distribution of the fading channel state, without any instantaneous CSIT, the performance limits are not fully known. The broadcast approach is investigated for the two-user MAC with *no* CSIT in [32]–[35]. In [32], the broadcast approach proposed in [10] is applied to the Gaussian slowly-fading MAC channel and average rates for the individual users are analyzed. In [33], the single-user broadcast approach is directly applied to the random access MAC with *no* CSIT, where the each user adpats its information layers to its own channel state. In [34] and [35], the same problem is studied, where in contrast to [33], the information layers of each transmitter are adapted to the *combined* state of the channels of all users, rendering a significantly larger achievable rate region. In this paper, we consider the two-user multiple access channel in which the transmitters have *local* CSI. Specifically, each channel randomly takes one of a finite number of states, and each transmitter only knows the state of its direct channel to the receiver *perfectly*, along with the probability distribution of the state of the other transmitter's channel. A similar model for the two-state MAC is considered in [36], in which a broadcast approach originally designed for the single-user channel is directly applied to the MAC. Specifically, in [36] each transmitter generates two coded layers, where each layer is adapted to one of the states of the channel linking the other transmitter to its receiver. This transmission approach is followed by successive decoding at the receiver in which there exists a pre-specified order of decoding of the information layers.

In this paper we consider the same channel model as in [36], i.e., the two-user MAC with *local* perfect CSIT, and propose a transmission and receiving strategies that differ from those of [36] in two ways. The first distinction is that we leverage the fact that the overall performance of the MAC is goverened by combined states of both channels. Hence, in contrast to [36], the information layers of each transmitter are adapted to the combined channel states (i.e., the direct as well as the interfering channels). The second distinction is that each transmitter, adaptively to the channel state, splits its messages to different numbers of information layers. Adaptively changing the number of information layers avoids causing unnecessary interference resulting from having undecoded information layers in some of the channel state.

We start by analyzing a two-state channel, and provide inner and outer bounds on the average capacity region of the rates that the users can sustain simultaneously. We also compare the resulting average achievable rate region with that of the approach in [36] to show the improvement gained from adapting the coded layers to the combined states of both transmitters' channels. In particular, encoding one additional information layer as the channel state gets stronger and employing the appropriate decoding order for each channel state results in improvement in the average achievable rate region when compared to that of the approach proposed in [36], in which the number of transmitted layers along with the decoding order are fixed and independent of the actual channel state. Furthermore, we prove that the proposed strategy achieves the sum-rate capacity asymptotically. We also provide the generalization of the proposed strategy to the case of any arbitrary finite number of channel states. Finally, the gains in the achievable rates are illustrated numerically in various settings. It is noteworthy that the improvement in the average achievable rate regions becomes more significant as the number of possible channel states increases. We also remark that our channel model subsumes the multiple access model of [37], which investigates a multi-access communication, in which the users get synchronized random access to the channel. User activities are random, and the set of active users is known only to the shared receiver. We will discuss the relevance of our model and proposed broadcast approach to those of [37] in details in Section IV-C.

The remainder of the paper is organized as follows. The finite-state channel model is presented in Section II. The rate-splitting and decoding strategy are provided in Section III for the two-state channel model. The corresponding achievable rate region and the outer bounds are delineated and compared in Section IV. Generalization of the proposed strategies to the finite-state channel is discussed in Section V, and the average achievable rate regions are numerically evaluated in Section VI. Section VII concludes the paper.

II. Channel Model

Consider the two-user fading MAC in which the channel input-output relationship is given by

$$Y = \sqrt{h_1}X_1 + \sqrt{h_2}X_2 + N, \tag{1}$$

where X_i is the signal of transmitter $i \in \{1, 2\}$ with an average transmission power constraint P_i over each block, h_i is the gain of the channel linking transmitter $i \in \{1, 2\}$ to the receiver, Y is the received signal, and N accounts for the additive white Gaussian noise with zero mean and unit variance. The random channel coefficients independently take one of $\ell \in \mathbb{N}$ distinct values denoted by $\{\alpha_m : m \in \{1, \ldots, \ell\}\}$.

Transmitter $i \in \{1, 2\}$ is assumed to know only the state of channel h_i, and the receiver is assumed to have access to the full CSI. Depending on the actual realization of the channel coefficients h_1 and h_2, the multiple access channel can be in one of ℓ^2 possible states. By leveraging the broadcast approach, the communication model in (1) can be equivalently

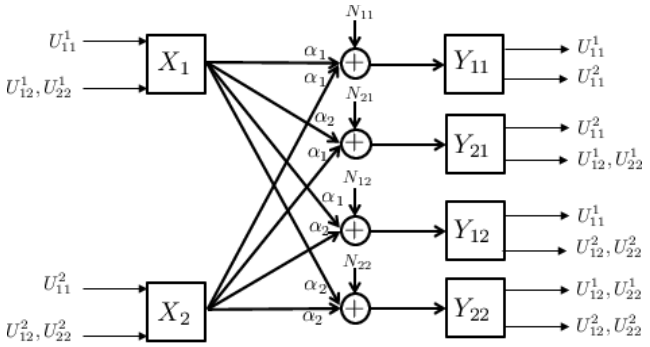

Fig. 1. Equivalent broadcast channel for the two-user MAC.

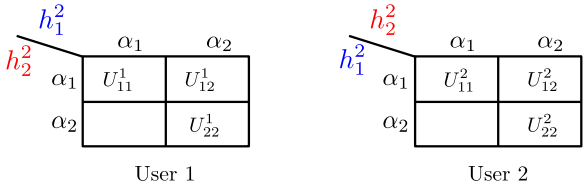

Fig. 2. Layering and codebook assignments.

presented by a broadcast network that has two inputs and ℓ^2 outputs, each corresponding to one channel combination. Figure 1 depicts the network model for $\ell = 2$. We denote the receiver corresponding to the combination $(h_1, h_2) = (\alpha_m, \alpha_n)$ by Y_{mn}, where

$$Y_{mn} = \alpha_m X_1 + \alpha_n X_2 + N_{mn}, \tag{2}$$

where N_{mn} is a zero-mean unit-variance Gaussian random variable. Without loss of generality, we assume that the channel gains $\{\alpha_m : m \in \{1, \ldots, \ell\}\}$ are ordered as $0 < \alpha_1 < \cdots < \alpha_\ell < +\infty$. We define p_{mn} as the probability of the state $(h_1, h_2) = (\alpha_m, \alpha_n)$. Accordingly, we also define $q_m \triangleq \sum_{n=1}^{\ell} p_{mn}$ and $p_n \triangleq \sum_{m=1}^{\ell} p_{mn}$. For convenience in notations, we will focus throughout the paper on the case of symmetric average transmission power constraints, i.e., $P_1 = P_2 = P$, whereas the generalization to the case of asymmetric power constraints is straightforward. Finally, throughout the paper we use the notation $C(x, y) \triangleq \frac{1}{2}\log_2(1 + \frac{x}{\frac{1}{P}+y})$.

III. Rate Splitting and Decoding Schemes

In this section, we focus on the two-state channel ($\ell = 2$) and we will discuss the general case of multi-state channels for any arbitrary $\ell \geq 2$ in Section V. In order to furnish a context for comparisons with the existing literature, and to illustrate the novel aspects of the proposed codebook assignment and decoding scheme, we first summarize the broadcast approach of [36] in Subsection III-A. Throughout this section, we refer to channel states α_1 and α_2 as the *weak* and *strong* channels, respectively.

A. Overview: Fixed Layering

According to the proposed approach in [36], in channel state α_m, transmitter i splits its message to two information layers via two independent codebooks denoted by T_{m1}^i and T_{m2}^i. The rate of layer T_{m1}^i is adapted to the *weak* channel state of the other user while the rate of layer T_{m2}^i is adapted to the *strong* channel state. Thus, each transmitter encodes its information stream by two layers and adapts the distribution of power between them according to its own channel state. Subsequently, the receiver implements a sequential decoding approach according to which it decodes one layer from transmitter 1 followed by one layer from transmitter 2, and then the remaining layer of transmitter 1, and finally the remaining layer of transmitter 2. This order is pre-fixed and is used in all channel states.

B. State-Dependent Layering

Due to both direct and interfering roles of each transmitter, the rates of the transmitted information streams need to be adapted to the combined state of both transmitters' channels. Furthermore, by leveraging the available partial CSIT, each transmitter can opportunistically sustain higher rates by adapting its transmission layers to the instantaneous state of its own channel.

Based on these two observations, we propose to dynamically split the message of each transmitter into independent codebooks depending on the actual state of the channel known to the transmitter. Specifically, when transmitter $i \in \{1, 2\}$ is in the *weak* state, we encode its messaged by only one layer denoted by U_{11}^i. On the other hand, when transmitter $i \in \{1, 2\}$ is in the *strong* state, it splits its data stream into two layers denoted by U_{12}^i and U_{22}^i. Based on this layering approach, codebook U_{12}^i (or U_{22}^i) is adapted to the state in which the other transmitter experiences a *weak* (or *strong*) channel. The details of information layering and assigning codebooks to different channel states are depicted in Fig. 2. In this figure, the cell corresponding to the combined state (α_m, α_n) for $m, n \in \{1, 2\}$ specifies which codebook is adapted to that state.

We remark that the hallmark of the broadcast approach is ordering the virtual receivers corresponding to the different combined channel states based on their relative degradedness. Defining degradedness is straightforward for the single-user channel (e.g., the receiver corresponding to the weak channel is degraded with respect to the receiver corresponding to the strong channel. In MAC, in contrast, there is no natural notion of degradedness, and any ordering is at least partly heuristic. In our proposed approach, the underpinning way of ordering the receivers is as follows: when the state of either transmitter 1 or 2 changes from the *weak* to the *strong* state, the receiver affords to decode an extra information layer. Corresponding to each channel state, the receiver decodes all the layers generated by transmitters 1 and 2.

C. Decoding Scheme

We propose a decoding scheme based on which the total number of decodable codebooks increases as either one of the channels becomes stronger. In this decoding scheme, demonstrated in Table I, different combinations of the codebooks in different channel states are decoded as follows.

- **State** (α_1, α_1)**:** Both transmitters are in the *weak* state, and generate codebooks $\{U_{11}^1, U_{11}^2\}$ according to Fig. 2.

TABLE I
DECODING SCHEME

(h_1, h_2)	stage 1	stage 2
(α_1, α_1)	U_{11}^1, U_{11}^2	
(α_2, α_1)	U_{12}^1, U_{11}^2	U_{22}^1
(α_1, α_2)	U_{11}^1, U_{12}^2	U_{22}^2
(α_2, α_2)	U_{12}^1, U_{12}^2	U_{22}^1, U_{22}^2

In this state, the baseline layers U_{11}^1 and U_{11}^2 are jointly decoded.

- **State** (α_2, α_1)**:** When only the channel of transmitter 1 is *strong*, three codebooks $\{U_{12}^1, U_{22}^1, U_{11}^2\}$ are generated. As shown in Table I, codebooks $\{U_{12}^1, U_{11}^2\}$, which are adapted to the channel state (α_2, α_1) are jointly decoded, followed by decoding the remaining codebook U_{22}^1.
- **State** (α_1, α_2)**:** This state is similar to (α_2, α_1), except that the roles of transmitters 1 and 2 are swapped.
- **State** (α_2, α_2)**:** Finally, when both transmitters have *strong* channels, four codebooks are decoded in the order depicted in the last row of Table I. First, the baseline layers $\{U_{12}^1, U_{12}^2\}$ are jointly decoded, followed by jointly decoding $\{U_{22}^1, U_{22}^2\}$.

D. Advantages of State-Dependent Layering

Compared with a similar network with no CSIT investigated in [35], the major distinction is that the transmitters do not have a pre-fixed layering strategy, and each transmitter selects its layering approach dynamically, and based on the known instantaneous channel realization. Furthermore, the major distinction with a similar network with partial CSIT investigated in [36] is adapting the number of encoded layers proportionately to the strength of combined channel state. This key difference leads to two major advantages. The first advantage is that adapting the number of layers leads to having fewer number of encoded layers, which in turn, leads to reduced complexity in decoding and power allocation across different codebooks. The second advantage pertains to providing the receiver with the flexibility to vary the decoding order according to the combined channel state, which in turn results in higher degrees of freedom in optimizing power allocation, and subsequently larger rate regions. Specifically, as shown in Theorem 2 and in numerical evaluations, when power allocation is optimized to achieve the maximum sum-rate capacity, the achievable rate region of the proposed scheme subsumes that of [36], and as the number of channel states increases, the gap becomes even more significant. The number of codebooks required in our approach is $\frac{\ell(\ell+1)}{2}$, whereas [36] is ℓ^2 for the ℓ-state channel. Finally, depending on the actual channel state, our approach decodes between 2 and $\frac{\ell(\ell+1)}{2}$ codebooks, whereas [36] always decodes ℓ^2 codebooks. Even though it might intuitively seem that the approach in [36] (using extra codebooks) is expected to subsume our proposed scheme simply by allocating zero power to the additional codebooks, this in fact is not the case. The key determing factor behind this improvement in our achievable regions, as shown through out the paper, is the *varying* decoding order of the received codebooks, showing that fixing the decoding order in all possible channel states (as assumed in [36]) is not universally optimal.

It is noteworthy that the two-state channel model in Fig. 1 with channel states $\alpha_1 = 0$ and $\alpha_2 = 1$ reduces to the two-user Gaussian channel with random access studied in [37]. In this special case, it can be shown that reserving one codebook to be decoded exclusively in each of the interference-free states, i.e., (α_1, α_2) and (α_2, α_1), enlarges the achievable rate region. Hence, it is beneficial in this special case to treat codebooks (U_{22}^1, U_{22}^2) as interference whenever both users are active, i.e., channel state (α_2, α_2). In other words, channel state (α_2, α_2) becomes degraded with respect to each of channel states (α_1, α_2) and (α_2, α_1). Nonetheless, in general, in the constant presence of interference, i.e., $\alpha_1 > 0$, reserving two codebooks to be decoded exclusively in these two channel states limits the average achievable rate region.

IV. INNER AND OUTER BOUNDS ON THE CAPACITY REGION

We are interested in delineating the average capacity region, calculated over a sufficiently large number of independent fading blocks. In this section, we provide inner and outer bounds on the average capacity region for the proposed codebook assignment and decoding scheme. For this purpose, we define $R_i(h_1, h_2)$ as the rate of transmitter i for the state pair (h_1, h_2). Accordingly, we define $\bar{R}_i \triangleq \mathbb{E}_{h_1,h_2}[R_i(h_1, h_2)]$ as the *average* rate of transmitter i, where the expected value is with respect to the distributions of h_1 and h_2. Hence, the average capacity region is the convex hull of all achievable average rates $(\bar{R}_1, \bar{R}_2)$.

A. Average Achievable Rate Region

We define $\beta_{ij}^k \in [0, 1]$ as the fraction of the total power P assigned to information layer U_{ij}^k, where for every $j, k \in \{1, 2\}$ we have $\sum_{i=1}^{j} \beta_{ij}^k = 1$. In the next theorem, we provide an average achievable rate region, that is an inner bound for the average capacity region.

Theorem 1 (Average Achievable Region): For the codebook assignment in Fig. 2, and the decoding scheme in Table I, for any given set of power allocation factors $\{\beta_{ij}^k\}$, the average achievable rate region $\{\bar{R}_1, \bar{R}_2\}$ is the set of all rates that satisfy

$$\begin{aligned}\bar{R}_1 \leq\, & q_1 C\left(\alpha_1, \alpha_2\beta_{22}^2\right) \\ & + q_2\left(C\left(\alpha_2\beta_{12}^1, \alpha_2\beta_{22}^1 + \alpha_2\beta_{22}^2\right) + C\left(\alpha_2\beta_{22}^1, 0\right)\right),\end{aligned} \tag{3}$$

$$\begin{aligned}\bar{R}_2 \leq\, & p_1 C(\alpha_1, \alpha_2\beta_{22}^1) \\ & + p_2\left(C\left(\alpha_2\beta_{12}^2, \alpha_2\beta_{22}^1 + \alpha_2\beta_{22}^2\right) + C\left(\alpha_2\beta_{22}^2, 0\right)\right),\end{aligned} \tag{4}$$

$$\begin{aligned}\bar{R}_1 + \bar{R}_2 \leq\, & q_1 p_1 C\left(2\alpha_1, 0\right) \\ & + q_1 p_2 C\left(\alpha_1 + \alpha_2\beta_{12}^2 + \alpha_2\beta_{22}^2, 0\right) \\ & + q_2 p_1 C\left(\alpha_1 + \alpha_2\beta_{12}^1 + \alpha_2\beta_{22}^1, 0\right) \\ & + q_2 p_2 C\left(\alpha_2\beta_{12}^1 + \alpha_2\beta_{12}^2 + \alpha_2\beta_{22}^1 + \alpha_2\beta_{22}^2, 0\right).\end{aligned} \tag{5}$$

Proof: See Appendix A. ■

The theorem above specifies the average achievable rate region for a specific decoding order. It is noteworthy that by relaxing the order, we can allow the receivers to dynamically deploy different decoding orders in the four possible channel states. Consequently, in any given channel state (α_m, α_n) for $m, n \in \{1, 2\}$, the set of transmitted layers along with the receiver constitute a multiple access channel with $(m+n)$ virtual independent transmitters (codebooks), in which, the vertices of the average achievable region can be achieved by employing time-sharing among all possible $(m+n)!$ decoding orders. Finally, between all four states (α_m, α_n) for $m, n \in \{1, 2\}$, the receiver can employ $\prod_{m,n}(m+n)!$ different possible decoding orders. Characterizing the average rate region for any of such decoding orders follows the same lines as in the proof of Theorem 1.

The region characterized in Theorem 1 is corresponding to the decoding order described in Table I, according to which the receiver decodes at most two codebooks at each stage until all the received codebooks from both transmitters are decoded. Despite the fact that limiting the number of jointly decoded codebooks at each stage is expected to result in a reduced rate region, it can be readily verified that the rate region achievable by employing a fully joint decoding scheme can be recovered via a time-sharing among the average achievable rates corresponding to all possible decoding orders in each channel state. This observation follows from the fact that at each state the codebooks to be decoded, being independently generated, form a MAC, for which it is well-understood that successive decoding achieves the same region as joint decoding. By leveraging the fact that in our proposed scheme the receiver is allowed to vary the decoding order in each channel state, next we show that under an appropriate decoding order, when we aim to maximize the sum-rate, the layering scheme proposed in Section III-B subsumes that of [36], as formalized next.

Theorem 2: For the two-user MAC channel with partial CSIT, when power allocations are set to maximize the sum-rate, the average rate region achievable by the layering scheme in Fig. 2 and the appropriate decoding order subsumes the rate region achieved in [36].

Proof: See Appendix B. ■

B. Outer Bounds

In this subsection, we provide two outer bounds on the average capacity region. Then, we compare the average achievable rate region characterized in Subsection IV-A with these two outer bounds.

1) Outer Bound 1: The first outer bound is the average capacity region corresponding to the two-user MAC in which the transmitters have complete access to the CSI [38]. This region is specified by OTVYZO in Fig. 3, and the corner points are specified in Appendix C.

2) Outer Bound 2: The second outer bound is the average capacity region of the two-user MAC with local CSI at transmitter 1 and full CSI at transmitter 2. Outer bound 2 is formally characterized in Theorem 3.

Theorem 3 (Outer Bound 2): For the two-user MAC with local CSI at transmitter 1 and full CSI at transmitter 2, the average capacity region is the set of all average rates enclosed by the region OTUWYZO *shown in Fig. 3, where the corner points are specified in Appendix C.*

Proof: See Appendix D. ■

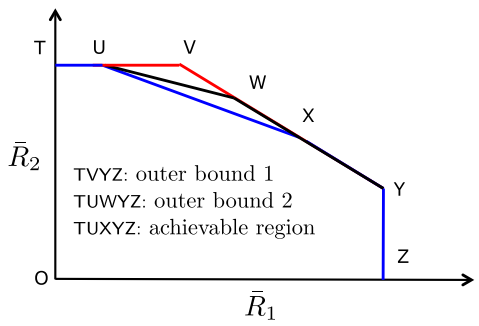

Fig. 3. Outer bounds on the average achievable rate region.

For the case of available local CSI at transmitter 1 and full CSI at transmitter 2, it can be shown that deploying the proposed layering scheme at transmitter 1(with local CSIT) achieves the average sum-rate capacity of Outer bound 1. This is formalized in the following theorem.

Theorem 4: With local CSI at transmitter 1 and full CSI at transmitter 2, an average achievable rate region is the region OTUXYZO *shown in Fig. 3. The average capacity region is achieved along* TU *and* YZ*, and the sum-rate capacity is achieved on* XY*. The corner points are specified in Appendix C.*

Proof: See Appendix E. ■

In Fig. 3, the region enclosed by OTVYZO is the average capacity region of a two-user MAC with full CSI at each transmitter (outer bound 1), which encloses outer bound 2. Parts of outer bound 2 described in Theorem 4, i.e., TU and XYZ, coincide with the average capacity region of the case of the two-user MAC with full CSIT. Specifically, along the line XY, the average sum-rate capacity is achieved for the channel even though one of the two transmitters has only local CSI. It can be shown that if both transmitters possess local CSI, it is possible to achieve an expected sum-rate that is close to outer bound 1, and the sum-rate capacity is achieved asymptotically for low and high power regimes. This result is formalized in Theorem 5.

Theorem 5 (Asymptotic Average Capacity Region): By adopting the codebook assignment presented in Section III, and setting $\beta_{22}^1 = \beta_{22}^2 = \frac{\alpha_1}{\alpha_2}$*, the sum-rate capacity of a two-user MAC with full CSIT is achievable asymptotically as* $P \to 0$ *or* $P \to \infty$.

Proof: See Appendix F. ■

C. Discussions on Layering

By setting $(\alpha_1, \alpha_2) = (0, 1)$ our channel model subsumes the random access model investigated in [37]. Specifically, [37] considers a Gaussian multiple access channel in which the transmitters are active with a certain probability, and independently of each other. In the two-user channel, this renders a setting in which each transmitter is only aware of its binary state, where the active users can be considered

TABLE II
SUCCESSIVE DECODING STAGES FOR $\ell-$STATE MAC WITH LOCAL CSIT

h_2 \ h_1	α_1	α_2	$\cdots$	α_q	$\cdots$	α_ℓ
α_1	U_{11}^1 U_{11}^2	U_{12}^1, U_{22}^1 $\mathcal{V}_{11}^2$	$\cdots$	$\cdot$	$\cdots$	$U_{1\ell}^1, \ldots, U_{\ell\ell}^1$ $\mathcal{V}_{(\ell-1)1}^2$
α_2	$\mathcal{V}_{11}^1$ U_{12}^2, U_{22}^2	$\mathcal{V}_{12}^1$ $\mathcal{V}_{21}^2$	$\cdots$	$\cdot$	$\cdots$	$\mathcal{V}_{1\ell}^1$ $\mathcal{V}_{2(\ell-1)}^2$
$\cdot$	$\cdot$	$\cdot$	$\cdots$	$\cdot$	$\cdots$	$\cdot$
α_p	$\cdot$	$\cdot$	$\cdots$	$\mathcal{V}_{(p-1)q}^1$ $\mathcal{V}_{p(q-1)}^2$	$\cdots$	$\cdot$
$\cdot$	$\cdot$	$\cdot$	$\cdots$	$\cdot$	$\cdots$	$\cdot$
α_ℓ	$\mathcal{V}_{(\ell-1)1}^1$ $U_{1\ell}^2, \ldots, U_{\ell\ell}^2$	$\mathcal{V}_{(\ell-1)2}^1$ $\mathcal{V}_{1\ell}^2$	$\cdots$	$\cdot$	$\cdots$	$\mathcal{V}_{(\ell-1)\ell}^1$ $\mathcal{V}_{(\ell-1)\ell}^2$

to be in the strong channel state $\alpha_2 = 1$ and the inactive users be in the weak channel state $\alpha_1 = 0$. This study also extends this two-state model for the transmitters to the general multi-user case. While channel models in this special case are the same, the encoding and decoding schemes are distinct. Comparing the layering and encoding strategies proposed in our paper with those of [37] sheds light on two important issues discussed next.

1) Ordering Channels' Degradedness: When we have assigned only one codebook (layer) to each transmitter, clearly the channel combination (α_1, α_1) is degraded with respect to (α_2, α_1) and (α_1, α_2), where both in turn are degraded with respect to (α_2, α_2). This is due to the fact that as a channel becomes stronger the achievable sum-rate increases. On the other hand, when we have multiple layers per transmitter (as is the case in this paper) considering a specific degradedness not only depends on the channels strengths, but also it depends on the decoding scheme adopted, which specifies which layers are discarded as noise in each channel combination. Such discarded codebooks, clearly cause interference. Hence, ordering the channel combinations based on their degradedness lies at the core of designing a broadcast approach. The major distinction between our proposed approach and that of [37] boils down to how the channel combinations are ordered. Specifically, in our approach we do not have any order of degradedness, while in [37] channel combination $(1, 1)$ can be naturally considered degraded with respect to channel combinations $(0, 1)$ and $(1, 0)$. This is due to the fact that a transmitter with channel gain 0 will not be imposing any interference on the other transmitter, while when both channels are non-zero, the transmitters will be interfering. Hence, from the perspectives of transmitters 1 and 2, channel $(1, 1)$ is degraded with respect to the channel combinations $(1, 0)$ and $(0, 1)$, respectively. It is noteworthy that for the special channel $(\alpha_1, \alpha_2) = (0, 1)$ the approach of [37] yields a slightly higher average sum-rate compared to our approach for this setting. In general, however, when the weak channel is non-zero, our approach outperforms (significantly). This is due to the fact that the approach of [37] is adapted to the special channel $(\alpha_1, \alpha_2) = (0, 1)$.

2) Optimal Layering: Increasing the number of layers, in general, is not necessarily an optimal approach. For instance, in [37] each transmitter is active with probability p independently of the rest. This indicates that in a large network consisting of M transmitters, with a high probability Mp users are active, and each transmitter knows its state. Hence, in the asymptote of $M \to \infty$, the network reduces to an Mp-user MAC where each transmitter has full CSI, in which case allocating only one layer to each transmitter is optimal. This observation is also verified in [37] where it is shown that one layer per transmitter is efficient in the multi-user case.

V. MULTI-STATE CHANNEL ($\ell \geq 2$)

In this section, we generalize the encoding and decoding strategy proposed in Section III for the case of two-state channel to the general ℓ-state channel, where $\ell \in \mathbb{N}$. When the channels have ℓ possible states, each transmitter is allocated ℓ different sets of codebooks, one corresponding to each channel state. Specifically, corresponding to channel state α_m for $m \in \{1, \ldots, \ell\}$, transmitter i encodes its message via m information layers generated according to independent codebooks. This set of codebooks is denoted by $\mathcal{W}_m^i \triangleq \{U_{1m}^i, \ldots, U_{mm}^i\}$.

Table II specifies the designation of the codebooks to different combined channel states. In this table, the channels are ordered in the ascending order. In particular, varying channels for transmitter 1, the combined channel state (α_q, α_p) precedes all channel states (α_k, α_p) for all $k > q$. Similarly, for transmitter 2 channel state (α_q, α_p) precedes the channel state (α_q, α_k), for every $k > p$. Furthermore, according to this approach, when user i's channel becomes stronger, it decodes additional codebooks. The sequence of decoding the codebooks, as shown in Table II, is specified in three steps:

1) State (α_1, α_1): We start by the weakest channel combination (α_1, α_1), and reserve the baseline codebooks U_{11}^1, U_{11}^2 to be the only codebooks to be decoded in this

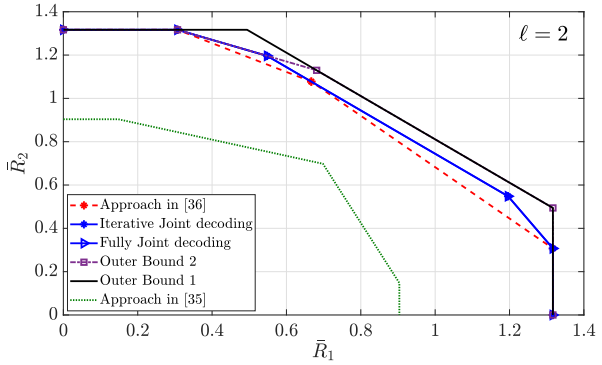

Fig. 4. Average rate regions for $\ell = 2$.

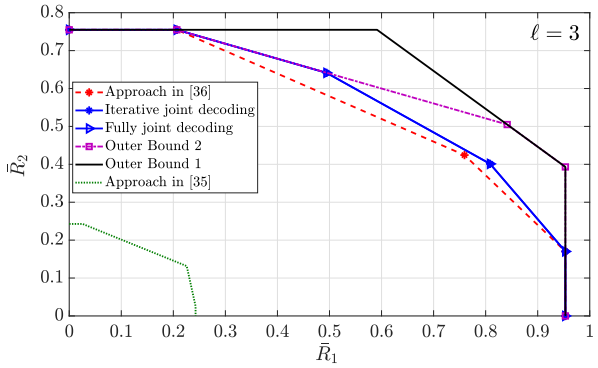

Fig. 5. Average rate regions for $\ell = 3$.

state. We define $\mathcal{V}_{11}^i \triangleq \{U_{11}^i\}$ as the set of codebooks that the receiver decodes from transmitter i when the channel state is (α_1, α_1).

2) States (α_1, α_q) and (α_q, α_1): Next, we construct the first row of the table, for this purpose we define $\mathcal{V}_{1q}^2$ as the set of the codebooks that the receiver decodes from transmitter 2, when the channel state is (α_1, α_q). Based on this, we can recursively specify the set of codebooks in each state. Specifically, in the state (α_1, α_q), we decode what has been decoded in the preceding state (α_1, α_{q-1}), i.e., the set of codebooks $\mathcal{V}_{1(q-1)}^2$, plus new codebooks $\{U_{1q}^1, \ldots, U_{qq}^1\}$. We construct the first column of the table in a similar fashion, except that the roles of transmitter 1 and 2 are swapped.

3) States (α_q, α_p) for $p, q > 1$: By defining the set of codebooks that the receiver decodes from transmitter i in the state (α_q, α_p) by $\mathcal{V}_{qp}^i$, the codebooks decoded in this state are related to the ones decoded in two preceding states. Specifically, in state (α_q, α_p) we decode codebooks $\mathcal{V}_{(p-1)q}^1$ and $\mathcal{V}_{p(q-1)}^2$. For example, for $\ell = 3$, the codebooks decoded in (α_2, α_3) includes those decoded for transmitter 1 in state (α_2, α_2) along with those decoded for transmitter 2 in channel state (α_1, α_3).

The decoding order in the general case is similar the one used for $\ell = 2$ in Table I. In particular, in channel state (α_q, α_p) the receiver successively decodes q codebooks from transmitter 1 along with p codebooks from transmitter 2. The set of decodable codebooks in channel state (α_q, α_p) is related to set of codebooks decoded for transmitter 2 in state (α_{q-1}, α_p) and those decoded for transmitter 1 (α_q, α_{p-1}).

The average achievable rate region for the codebook assignment and decoding strategy presented in this section is summarized in Theorem 6. Similar to the two-state channel case, we define $\beta_{mn}^i \in [0, 1]$ as the fraction of power allocated to the codebook U_{mn}^i such that $\sum_{m=1}^n \beta_{mn}^i = 1, \forall n \in \{1, \ldots \ell\}$.

Theorem 6 (General Rate Region): For the codebook assignment in Section V, and the decoding scheme in Table II, for any given set of power allocation factors $\{\beta_{mn}^i\}$, the average achievable rate region $\{\bar{R}_1, \bar{R}_2\}$ for the ℓ-state channel is the set of all rates that satisfy

$$\bar{R}_2 \leq \mathbb{E}[r_1(n, m)], \tag{6}$$

$$\bar{R}_2 \leq \mathbb{E}[r_2(n, m)], \tag{7}$$

$$\bar{R}_1 + \bar{R}_2 \leq \mathbb{E}[\min\{r_3(n, m), r_4(n, m)\}], \tag{8}$$

where the functions $\{r_1(n, m), \ldots, r_4(n, m)\}$, for all $m, n \in \{1, \ldots, \ell\}$ are defined in Appendix G.

VI. Numerical Evaluations

In this section, we illustrate the gains attained by the proposed leyring and decoding scheme through numerically evaluating the average achievable rates characterized in sections IV and V, for the two- and three-state channel models. We begin by evaluating the average rate region achievable by the proposed layering scheme in figures 4 and 5. In particular, we compare the average rate regions with the outer bounds established in Section IV-B, i.e., outer bound 1 (full CSI at both transmitters) and outer bound 2 (full CSI at transmitter 2 only). Furthermore, we evaluate the average achievable rate region corresponding to the encoding and decoding approach proposed in [36] for the same channel settings to demostarate the gleaned gains. Finally, we illustrate the role of the partially available CSIT incorporated in the proposed approach by comparing the average rate regions with that of the approach proposed in [35] for the two-user MAC with no CSIT.

For the two-state channel, Fig. 4 demonstrates the average rate region for $P_1 = P_2 = P = 10$ dB, channel gains $\alpha_1 = 0.25$, $\alpha_2 = 1$, and the channel probability parameters $q_1 = p_1 = 0.5$. It is observed that the rate region achievable by the decoding approach proposed in Section III coincides with that achieved by full joint decoding. According to the proposed layering scheme, each transmitter transmits three independent codebooks compared to four codebooks in the approach in [36]. Hence, the proposed decoding scheme gleans higher average sum-rate with fewer number of encoded layers which simplifies the possible search space for the appropriate power allocation and decoding order.

Similarly, for the three-state channel, Fig. 5 demonstrates the average rate region for channel gains $\alpha_1 = 0.04$, $\alpha_2 = 0.25$, $\alpha_3 = 1$, and channel probability parameters $q_1 = 0.3, q_2 = 0.4$ for transmitter 1, and $p_1 = 0.6, p_2 = 0.1$ for transmitter 2. We remark that for the three-state channel, we have extended the strategy of [36], in which we get nine codebooks per transmitter. This is different from our proposed iterative joint decoding policy that requires only six codebooks

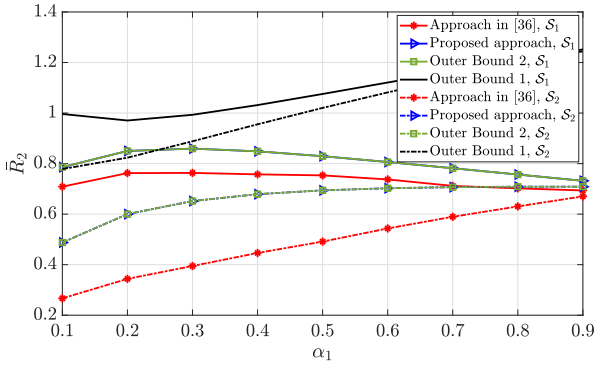

Fig. 6. Average rates of transmitter 2 for $\ell = 2$.

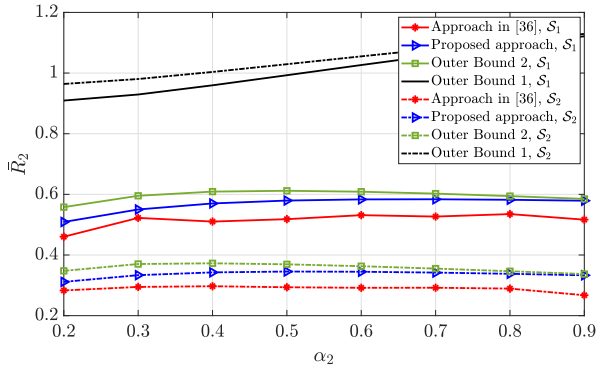

Fig. 7. Average rates of transmitter 2 for $\ell = 3$.

per transmitter. Hence, by adapting the number of codebooks as well as the decoding order to the combined channel state, the proposed strategy achieves higher average rates, while having lower encoding and decoding complexity.

In figures 6 and 7, we evaluate the achievable rates for user 1 and 2 under the following setting. First, we identify the corner point of the average achievable rate region at which transmitter 1 achieves the maximum average rate while the average sum-rate capacity is achieved by the two-users (corner point D on Fig. 10 in Appendix B). At this corner point, we evaluate the average achievable rate by user 2, $\bar{R}_2$, corresponding to the maximum achievable rate $\bar{R}_1$ in each of the proposed approach and the approach in [36]. Further, we evaluate the resulting $\bar{R}_2$ identified by outer bounds 1 and 2 that corresponds to the same $\bar{R}_1$. We consider two different settings to reflect the effect of symmetric/asymmetric average power constraints and channel probability distirbutions among the two users. In particular, the first setting denoted by $\mathcal{S}_1$, considers equal power constariants and symmetric channel distributions, while setting $\mathcal{S}_2$ considers unequal power constraints and asymmetric channel distribution. In Fig. 6, for the two-state channel model and a fixed $\bar{R}_1$, we evaluate $\bar{R}_2$ achieved by our scheme, the scheme in [36], outer bound 1, and outer bound 2 for $\alpha_2 = 1$, $P_1 = P_2 = 10$dB, and $q_1 = p_1 = 0.3$ in setting $\mathcal{S}_1$ and $P_1 = 10$dB, $P_2 = 6.9$dB, $q_1 = 0.8$, and $p_1 = 0.4$ in $\mathcal{S}_2$. In Fig. 7, a similar comparison is demonestrated for the three-state channel for $\alpha_1 = 0.1$, $\alpha_3 = 1$, $P_1 = P_2 = 10$dB, $q_1 = p_1 = 0.6, q_2 = p_2 = 0.1$ in $\mathcal{S}_1$, and $P_1 = 7$dB, $P_2 = 10$dB, $q_1 = 0.3, p_1 = 0.6, q_2 = 0.3, p_2 = 0.2$ in $\mathcal{S}_2$. Figures 6 and 7 show that for various settings, the proposed approach outperforms the approach proposed in [36] while achieving outer bound 2 in certain cases.

Furthermore, we evaluate theorems 4 and 5 in figures 8 and 9, respectively. In Fig. 8, we evaluate the average achievable rate region OTUXYZ specified in Fig. 3 for three scenarios $\hat{\mathcal{S}}_1, \hat{\mathcal{S}}_2, \hat{\mathcal{S}}_3$. In all three scenarios, we fix the average power constraint to 10 dB, i.e. $P_1 = P_2 = P = 10$ dB, the channel states are given by $(\alpha_1, \alpha_2) = (0.3, 1)$. On the other hand, we vary the channel probability distribution among the three scenarios where we evaluate the symmetric case in $\hat{\mathcal{S}}_1$ with $q_1 = p_1 = 0.5$, and the asymmetric cases in $\hat{\mathcal{S}}_1, \hat{\mathcal{S}}_2$ with $q_1 = 0.2, p_1 = 0.8$ and $q_1 = 0.4, p_1 = 0.5$, respectively. This figures verifies the statement of Theorem 4 for different scenarios showing that the average capacity region of two-user MAC with full CSIT is partially achieved through the proposed encoding and decoding scheme when only one user had full CSIT. Finally, Theorem 5 is evaluated in Fig. 9 in the low and high signal-to-noise ratio regimes, i.e., $P \to 0$ or $P \to \infty$. In Fig. 9, we fix the channel probability distribution such that $q_1 = p_1 = 0.5$ while varying the average power constraint in five different scenarios. In particular, we set $P_2 = 10$ dB and $P_1 \in \{40, 30, 20\}$ dB in scenarios $\bar{\mathcal{S}}_1, \bar{\mathcal{S}}_2, \bar{\mathcal{S}}_3$, respectively. Further, scenarios $\bar{\mathcal{S}}_4$ and $\bar{\mathcal{S}}_5$ corresponds to $P_1 = P_2 = 0.1$ dB and $P_1 = 0.1, P_2 = 10$ dB, respectively. Fig. 9 confirms the statement of Theorem 5 showing that the average achievable sum-rates of the proposed scheme approaches the sum-rate capacity in the high or low signal-to-noise ratio regimes.

VII. Conclusion

In this paper, we have proposed a novel broadcast approach for the two-user multiple access channel over a slowly-fading channel with only local channel state information at the transmitters. In particular, each transmitter is assumed to know the complete state information of its own channel to the receiver, while being oblivious to the state of the other channel. Existing broadcast strategies for such a channel model adapt the number of codebooks designed at each transmitter, as well as their rates, to the state of its individual channel. The proposed approach, in contrast, adapts the design of the information layers to the combined states of the channels resulting from all the transmitters. Average achievable rate regions for the proposed approach have been characterized, demonstrating that the proposed approach and its associated achievable rate region subsume those of the existing approaches. Also, we have established that the proposed strategy achieves the sum-rate capacity in the asymptote of small and large transmission power. Furthermore, the proposed approach has lower encoding and decoding complexity. In addition to the attained gains in the average achievable rates, further investigating the delay performance of the proposed approach is an encouraging path, where promising results have been shown in the literature for broadcast approach in the single-user channel. Further studies include adapting the proposed broadcast approach to a slowly-fading channel with random multiple access as well as extending the results to the settings in which the

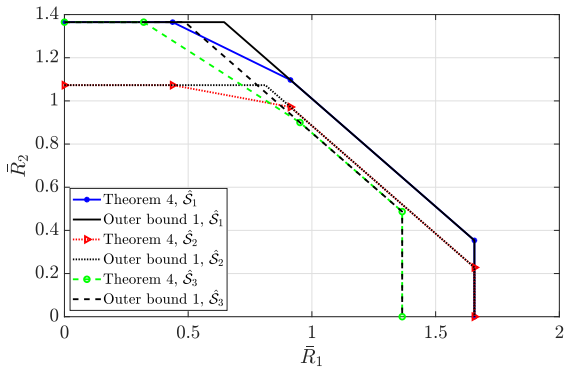

Fig. 8. Average rate regions in Theorem 4.

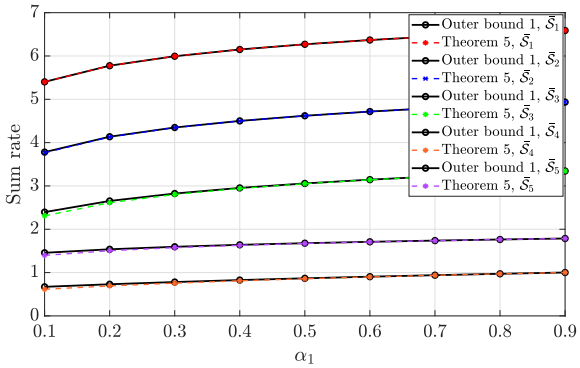

Fig. 9. Average sum-rates in Theorem 5.

channels follow a continuous fading model. Finally, we remark that depending on the relative channel conditions (e.g., when the weak channel's is 0) it is possible to have alternative broadcast approaches that render higher average sum-rate. This indicates that there is room to further investigate an optimized layering transmission for the model considered in this paper.

Appendix A
Proof of Theorem 1

It can be proved that for the successive decoding strategy outlined in Table I, the boundaries of the region outlined in Theorem 1 is achievable. First, we define the achievable rates of each codebook U_{ij}^k as R_{ij}^k, for $i \leq j, j, k \in \{1,2\}$. We start by considering the network state when both channels are weak. Transmitted message from transmitter i consists of U_{11}^i, for $i \in \{1,2\}$. In this state, the receiver jointly decodes all the received information layers U_{11}^1 and U_{11}^2. Successful decoding of these layers requires that individual rates and sum rates of jointly decoded codebooks are within a region bounded by a set of inequalities that defines the capacity region of a two-user MAC transmitting a single layer of information per transmitter.

Channel state (α_1, α_1):

$$R_{11}^1 \leq C\left(\alpha_1, 0\right) \triangleq \nu_{11}, \tag{9}$$
$$R_{11}^2 \leq C\left(\alpha_1, 0\right) \triangleq \eta_{11}, \tag{10}$$
$$R_{11}^1 + R_{11}^2 \leq C\left(2\alpha_1, 0\right) \triangleq \gamma_{11}. \tag{11}$$

By following the decoding order corresponding to channel states (α_1, α_2), (α_2, α_1), and (α_2, α_2), we follow the same steps to get the following set of rate constraints.

Channel state (α_1, α_2):

$$R_{11}^1 \leq C\left(\alpha_1, \alpha_2\beta_{22}^2\right) \triangleq \bar{\nu}_{11}, \tag{12}$$
$$R_{12}^2 \leq C\left(\alpha_2\beta_{12}^2, \alpha_2\beta_{22}^2\right) \triangleq \eta_{12}, \tag{13}$$
$$R_{11}^1 + R_{12}^2 \leq C\left(\alpha_1 + \alpha_2\beta_{12}^2, \alpha_2\beta_{22}^2\right) \triangleq \gamma_{12}, \tag{14}$$
$$R_{22}^2 \leq C\left(\alpha_2\beta_{22}^2, 0\right) \triangleq \eta_{22}. \tag{15}$$

Channel state (α_2, α_1):

$$R_{12}^1 \leq C\left(\alpha_2\beta_{12}^1, \alpha_2\beta_{22}^1\right) \triangleq \nu_{12}, \tag{16}$$
$$R_{11}^2 \leq C\left(\alpha_1, \alpha_2\beta_{22}^1\right) \triangleq \bar{\eta}_{11}, \tag{17}$$
$$R_{12}^1 + R_{11}^2 \leq C\left(\alpha_2\beta_{12}^1 + \alpha_1, \alpha_2\beta_{22}^1\right) \triangleq \gamma_{21}, \tag{18}$$
$$R_{22}^1 \leq C\left(\alpha_2\beta_{22}^1, 0\right) \triangleq \nu_{22}. \tag{19}$$

Channel state (α_2, α_2):

$$R_{12}^1 \leq C\left(\alpha_2\beta_{12}^1, \alpha_2\beta_{22}^1 + \alpha_2\beta_{22}^2\right) \triangleq \bar{\nu}_{12}, \tag{20}$$
$$R_{12}^2 \leq C\left(\alpha_2\beta_{12}^2, \alpha_2\beta_{22}^1 + \alpha_2\beta_{22}^2\right) \triangleq \bar{\eta}_{12}, \tag{21}$$
$$R_{12}^1 + R_{12}^2 \leq C\left(\alpha_2\beta_{12}^1 + \alpha_2\beta_{12}^2, \alpha_2\beta_{22}^1 + \alpha_2\beta_{22}^2\right) \triangleq \gamma_{22}, \tag{22}$$
$$R_{22}^2 \leq C\left(\alpha_2\beta_{22}^2, 0\right) \triangleq \bar{\eta}_{22}, \tag{23}$$
$$R_{22}^1 \leq C\left(\alpha_2\beta_{22}^1, 0\right) \triangleq \bar{\nu}_{22}, \tag{24}$$
$$R_{22}^1 + R_{22}^2 \leq C\left(\alpha_2\beta_{22}^1 + \alpha_2\beta_{22}^2, 0\right) \triangleq \bar{\gamma}_{22}. \tag{25}$$

Next, we aggregate the constraints on the rates (9)-(25) to characterize an average achievable rate region. We start by characterizing the aggregate achievable rate region for both transmitters in each channel state by using Fourier-Motkinz elimination (FME) [39, Appendix D]. To this end, note that $R_i(h_1, h_2)$ denotes the rate of transmitter i for the combined channel (h_1, h_2). For instance, when both channels are weak, then $R_i(h_1, h_2) = R_{11}^i$. As a result, the first combined channel state (α_1, α_1), is a straightforward case, in which we can directly replace R_{11}^i by $R_i(\alpha_1, \alpha_1)$ in (9)-(11). Hence,

$$R_1(\alpha_1, \alpha_1) \leq \nu_{11}, \quad R_2(\alpha_1, \alpha_1) \leq \eta_{11}, \tag{26}$$
$$R_1(\alpha_1, \alpha_1) + R_2(\alpha_1, \alpha_1) \leq \gamma_{11}. \tag{27}$$

For channel state (α_1, α_2), we directly follow the FME procedure to sequentially eliminate the layered random codebooks. First, in (16)-(25), we replace R_{11}^1 by $R_1(\alpha_1, \alpha_2)$, and replace R_{12}^2 by $(R_2(\alpha_1, \alpha_2) - R_{22}^2)$. Afterwards, we have one remaining variable to eliminate, i.e., R_{22}^2, which can be achieved by collecting all the inequalities that have the term R_{22}^2 with a negative sign resulting in (12) and (14). Finally, we add each of these equations to (23) (all the inequalities that contain R_{22}^2 with positive sign) resulting in

$$R_1(\alpha_1, \alpha_2) \leq \bar{\nu}_{11}, \quad R_2(\alpha_1, \alpha_2) \leq \eta_{12} + \eta_{22}, \tag{28}$$
$$R_1(\alpha_1, \alpha_2) + R_2(\alpha_1, \alpha_2) \leq \eta_{22} + \gamma_{12}. \tag{29}$$

Similar elimination steps can be followed for the codebooks decoded in channel state (α_2, α_1). After eliminating the auxiliary variables R_{12}^1, R_{22}^1, and R_{11}^2 by following standard FME

procedure, the achievable rate region for transmitters 1 and 2 in this channel state is given by

$$R_1(\alpha_2,\alpha_1) \le \nu_{12}+\nu_{22}, \quad R_2(\alpha_2,\alpha_1) \le \bar{\eta}_{11}, \tag{30}$$
$$R_1(\alpha_2,\alpha_1) + R_1(\alpha_2,\alpha_1) \le \gamma_{21}+\nu_{22}. \tag{31}$$

Finally, in channel state (α_2,α_2), the total achievable rates of transmitters 1 and 2 are bounded as follows.

$$R_1(\alpha_2,\alpha_2) \le \bar{\nu}_{12}+\bar{\nu}_{22}, \quad R_2(\alpha_2,\alpha_2) \le \bar{\eta}_{12}+\bar{\eta}_{12}, \tag{32}$$
$$R_1(\alpha_2,\alpha_2) + R_2(\alpha_2,\alpha_2) \le \gamma_{22}+\bar{\gamma}_{22}, \tag{33}$$
$$R_1(\alpha_2,\alpha_2) + R_2(\alpha_2,\alpha_2) \le \bar{\nu}_{12}+\bar{\eta}_{12}+\bar{\gamma}_{22}, \tag{34}$$
$$R_1(\alpha_2,\alpha_2) + R_2(\alpha_2,\alpha_2) \le \gamma_{22}+\bar{\nu}_{22}+\bar{\eta}_{22}, \tag{35}$$
$$2R_1(\alpha_2,\alpha_2) + R_2(\alpha_2,\alpha_2) \le \bar{\nu}_{12}+\gamma_{22}+\bar{\gamma}_{22}+\bar{\nu}_{22}. \tag{36}$$

As a result, the average achievable rate of transmitter i, i.e.,

$$\bar{R}_i = \mathbb{E}_{h_1,h_2}[R_i(h_1,h_2)] = \sum_{m,n} p_{mn} R_i(\alpha_m,\alpha_n), \tag{37}$$

is bounded by the average of the corresponding bounds in (26), (28), (30), and (32), i.e.,

$$\bar{R}_1 \le q_1 \min\{\nu_{11},\bar{\nu}_{11}\} + q_2 \min\{\nu_{12}+\nu_{22},\bar{\nu}_{12}+\bar{\nu}_{22}\}, \tag{38}$$
$$\bar{R}_2 \le p_1 \min\{\eta_{11},\bar{\eta}_{11}\} + p_2 \min\{\eta_{12}+\eta_{22},\bar{\eta}_{12}+\bar{\eta}_{22}\}. \tag{39}$$

Note that the $\min\{\cdot,\cdot\}$ terms in (38) and (39) are needed to guarantee the decodability of each codebook in two different channel states, e.g., rate of codebook U_{11}^1 must be achievable in each of channel states (α_1,α_1) and (α_1,α_2), even though it is primarily adapted to state (α_1,α_1). Codebooks U_{12}^1, U_{22}^1, U_{11}^2, U_{12}^2, and U_{22}^2 are required to satisfy similar conditions.

Similarly, by noting that given (32) and (33) the bound in (36) is redundant, the average sum-rate is bounded by the average of the bounds in (27), (29), (31), and (33)-(35) as follows.

$$\begin{aligned}\bar{R}_1+\bar{R}_2 \le\ & p_{11}\gamma_{11} + p_{12}(\gamma_{12}+\eta_{22}) + p_{21}(\gamma_{21}+\nu_{22}) \\ & + p_{22}\min\{\gamma_{22}+\bar{\gamma}_{22}, \\ & \bar{\nu}_{12}+\bar{\eta}_{12}+\bar{\gamma}_{22}, \gamma_{22}+\bar{\nu}_{22}+\bar{\eta}_{22}\}.\end{aligned} \tag{40}$$

Finally, we remark that by using (9), (12), (16), (20), (19), and (24) it can be readily verified that $\bar{\nu}_{11} \le \nu_{11}$, $\bar{\nu}_{12} \le \nu_{12}$, and $\bar{\nu}_{22} = \nu_{22}$, respectively. Similarly, by using (10), (17), (13), (21), (19), and (23) we have $\bar{\eta}_{11} \le \eta_{11}$, $\bar{\eta}_{12} \le \eta_{12}$, and $\bar{\eta}_{22} = \eta_{22}$. Additionally, according to (20)-(25), we have $\gamma_{22} \le \bar{\nu}_{12}+\bar{\eta}_{12}$ and $\bar{\gamma}_{22} \le \bar{\nu}_{22}+\bar{\eta}_{22}$. Therefore, the average rate region defined by (38)- (40) can be readily simplified to that outlined in Theorem 1.

APPENDIX B
PROOF OF THEOREM 2

The average rate region of our approach is the convex hull of all the average rate regions that are attained by different decoding orders in different states. In order to show that this region subsumes that of [36] we show the following properties:

1) Our rate region $(\bar{R}_1,\bar{R}_2)$ subsumes the rate region specified by OABCDEF in Fig. 10.
2) The approach of [36] has a rate region specified by OABC'EF in Fig. 10.

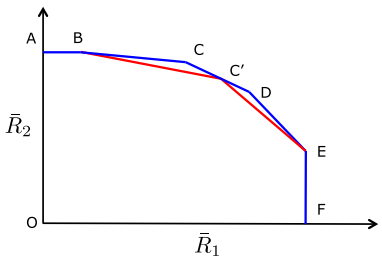

Fig. 10. Rate regions OABCDEF and OABC'EF.

3) The point C' lies on the segment CD in Fig. 10, strictly away from the corner points.

1- $(\bar{R}_1,\bar{R}_2)$ subsumes OABCDEF: This region can be achieved by time-sharing among the corner points A,B,C,D,E,F which we characterize next. Note that we follow the same notation defined in Appendix A where the rate of codebooks U_{ij}^k is denoted by R_{ij}^k, for $i \le j, j,k \in \{1,2\}$.

Corner A: By setting the rate of all the codebooks corresponding to transmitter 1 to 0, i.e. $R_{11}^1 = R_{12}^1 = R_{22}^1 = 0$, the maximum average achievable rate of transmitter 2 is given by

$$\bar{R}_2 \le p_1 C(\alpha_1,0) + p_2 C(\alpha_2,0). \tag{41}$$

Corner F: Alternatively, by setting the rate of all the codebooks corresponding to transmitter 2 to 0, i.e. $R_{11}^2 = R_{12}^2 = R_{22}^2 = 0$, the maximum average achievable rate of transmitter 1 is given by

$$\bar{R}_1 \le q_1 C(\alpha_1,0) + q_2 C(\alpha_2,0). \tag{42}$$

Corner B: At this corner, for every channel state (α_m,α_n) where $m,n \in \{1,2\}$, all the codebooks received from transmitter 1 are decoded and eliminated before decoding those received from transmitter 2 resulting in the following achievable rates for each user.

Channel state (α_1,α_1):

$$R_1(\alpha_1,\alpha_1) \le C(\alpha_1,\alpha_1), \quad R_2(\alpha_1,\alpha_1) \le C(\alpha_1,0). \tag{43}$$

Channel state (α_1,α_2):

$$R_1(\alpha_1,\alpha_2) \le C(\alpha_1,\alpha_2), \quad R_2(\alpha_1,\alpha_2) \le C(\alpha_2,0). \tag{44}$$

Channel state (α_2,α_1):

$$R_1(\alpha_2,\alpha_1) \le C(\alpha_2,\alpha_1), \quad R_2(\alpha_2,\alpha_1) \le C(\alpha_1,0). \tag{45}$$

Channel state (α_2,α_2):

$$R_1(\alpha_2,\alpha_2) \le C(\alpha_2,\alpha_2), \quad R_2(\alpha_2,\alpha_2) \le C(\alpha_2,0). \tag{46}$$

Hence, the average achievable rates for transmitters 1 and 2 at point B are given by

$$\bar{R}_1 \le q_1 C(\alpha_1,\alpha_2) + q_2 C(\alpha_2,\alpha_2), \tag{47}$$
$$\bar{R}_2 \le p_1 C(\alpha_1,0) + p_2 C(\alpha_2,0). \tag{48}$$

Corner E: The decoding scheme of point E is similar to that stated for point B except that the roles of transmitters 1 and 2 are swapped, resulting in

$$\bar{R}_2 \le p_1 C(\alpha_1,\alpha_2) + p_2 C(\alpha_2,\alpha_2), \tag{49}$$

TABLE III
SUCCESSIVE DECODING ORDER ACHIEVING SUM-RATE CAPACITY

(h_1, h_2)	stage 1	stage 2	stage 3	stage 4
(α_1, α_1)	U_{11}^2	U_{11}^1		
(α_2, α_1)	U_{12}^1	U_{11}^2	U_{22}^1	
(α_1, α_2)	U_{12}^2	U_{22}^2	U_{11}^1	
(α_2, α_2)	U_{12}^2	U_{12}^1	U_{22}^2	U_{22}^1

TABLE IV
SUCCESSIVE DECODING SCHEME IN [36]

(h_1, h_2)	stage 1	stage 2	stage 3	stage 4
(α_1, α_1)	T_{11}^1	T_{11}^2	T_{12}^1	T_{12}^2
(α_1, α_2)	T_{11}^1	T_{21}^2	T_{12}^1	T_{22}^2
(α_2, α_1)	T_{21}^1	T_{11}^2	T_{22}^1	T_{12}^2
(α_2, α_2)	T_{21}^1	T_{21}^2	T_{22}^1	T_{22}^2

$$\bar{R}_1 \leq q_1 C(\alpha_1, 0) + q_2 C(\alpha_2, 0). \tag{50}$$

Corner D: This corner can be achieved by following the successive decoding order in Table III under the power allocation $\beta_{22}^2 = \beta_{22}^1 = \frac{\alpha_1}{\alpha_2}$. The achievable rates for transmitter 1 and 2 are

Channel state (α_1, α_1):

$$\begin{aligned} R_2(\alpha_1, \alpha_1) &= R_{11}^2 \leq C(\alpha_1, \alpha_1), \\ R_1(\alpha_1, \alpha_1) &= R_{11}^1 \leq C(\alpha_1, 0). \end{aligned} \tag{51}$$

Channel state (α_2, α_1):

$$R_2(\alpha_2, \alpha_1) = R_{11}^2 \leq C(\alpha_1, \alpha_1), \tag{52}$$

$$\begin{aligned} R_1(\alpha_2, \alpha_1) &= R_{12}^1 + R_{22}^1 \\ &\leq C(\alpha_2 \beta_{12}^1, \alpha_1 + \alpha_2 \beta_{22}^1) + C(\alpha_2 \beta_{22}^1, 0). \end{aligned} \tag{53}$$

Channel state (α_1, α_2):

$$R_1(\alpha_1, \alpha_2) = R_{11}^1 \leq C(\alpha_1, 0), \tag{54}$$

$$\begin{aligned} R_2(\alpha_1, \alpha_2) &= R_{12}^2 + R_{22}^2 \\ &\leq C(\alpha_2 \beta_{12}^2, \alpha_1 + \alpha_2 \beta_{22}^1) + C(\alpha_2 \beta_{22}^2, \alpha_1). \end{aligned} \tag{55}$$

Channel state (α_2, α_2):

$$\begin{aligned} R_1(\alpha_2, \alpha_2) &= R_{12}^1 + R_{22}^1 \\ &\leq C(\alpha_2 \beta_{12}^1, \alpha_2 + \alpha_2 \beta_{22}^1) + C(\alpha_2 \beta_{22}^1, 0), \end{aligned} \tag{56}$$

$$\begin{aligned} R_2(\alpha_2, \alpha_2) &= R_{12}^2 + R_{22}^2 \\ &\leq C(\alpha_2 \beta_{12}^2, \alpha_1 + \alpha_2 \beta_{22}^1) + C(\alpha_2 \beta_{22}^2, \alpha_1). \end{aligned} \tag{57}$$

Hence, by directly substituting the power allocation $\beta_{22}^2 = \beta_{22}^1 = \frac{\alpha_1}{\alpha_2}$, in (52)-(57), the average achievable rates for transmitters 1 and 2 at point D are given by

$$\begin{aligned} \bar{R}_1 &= C(\alpha_1, 0) + q_2 C(\alpha_2 - \alpha_1, \alpha_1 + \alpha_1), \\ \bar{R}_2 &= C(\alpha_1, \alpha_1) + p_2 C((\alpha_2 - \alpha_1), \alpha_1 + \alpha_2). \end{aligned} \tag{58}$$

Corner C: We follow the same decoding order as in Table III except that the roles of transmitters 1 and 2 are swapped. Hence

$$\begin{aligned} \bar{R}_2 &= C(\alpha_1, 0) + p_2 C(\alpha_2 - \alpha_1, \alpha_1 + \alpha_1), \\ \bar{R}_1 &= C(\alpha_1, \alpha_1) + q_2 C((\alpha_2 - \alpha_1), \alpha_1 + \alpha_2). \end{aligned} \tag{59}$$

2- ABC'EF is the average rate region of [36]: According to the approach presented in [36], the rate region enclosed by the points A,B,C',E,F are achieved by varying the power allocation among the transmitted codebook according to the fixed decoding order specified in IV.

3- C' lies on CD: We first show that both our approach and the approach of [36] achieve the sum-rate capacity, established in [29]. Then we show that the point C (D) appears strictly on the right (left) side of of C'. For this purpose, we first remark that [29, Theorem 13] provides a power allocation algorithm according to which for any $\rho \in [C(\alpha_1, \alpha_1), C(\alpha_1, 0)]$ the average sum-rate capacity is achieved, in which case the rates satisfy:

$$\min\{R_1(\alpha_1, \alpha_1), R_1(\alpha_1, \alpha_2)\} = \rho, \tag{60}$$

$$\min\{R_2(\alpha_1, \alpha_1), R_2(\alpha_2, \alpha_1)\} = C(\alpha_1 + \alpha_1, 0) - \rho, \tag{61}$$

$$\begin{aligned} \min\{R_1(\alpha_2, \alpha_1), R_1(\alpha_2, \alpha_2)\} &= C(\alpha_2 + \alpha_1, 0) \\ &\quad - \min\{R_2(\alpha_1, \alpha_1), \\ &\quad R_2(\alpha_2, \alpha_1)\}, \end{aligned} \tag{62}$$

$$\begin{aligned} \min\{R_2(\alpha_1, \alpha_2), R_2(\alpha_2, \alpha_2)\} &= C(\alpha_2 + \alpha_2, 0) \\ &\quad - \min\{R_1(\alpha_2, \alpha_1), \\ &\quad R_1(\alpha_2, \alpha_2)\}. \end{aligned} \tag{63}$$

Next, we show that all the average rates on the segment CD achieve the average sum-rate capacity. Specifically, from (52)-(57), the rates achievable by codebooks $\{U_{11}^i, U_{12}^i, U_{22}^i\}$ are

$$R_{11}^1 = C(\alpha_1, 0), \quad R_{11}^2 = C(\alpha_1, \alpha_1), \tag{64}$$

$$R_{12}^1 = C((\alpha_2 - \alpha_1), \alpha_1 + \alpha_1), \quad R_{22}^1 = C(\alpha_1, 0), \tag{65}$$

$$R_{12}^2 = C((\alpha_2 - \alpha_1), \alpha_1 + \alpha_2), \quad R_{22}^2 = C(\alpha_1, \alpha_1). \tag{66}$$

It can be readily verified that the rates in (64)-(66) are the same as those specified in (60)-(63) when we set $\rho = C(\alpha_1, 0)$. Similarly, the rate achieved at point C achieve the rates in (60)-(63) for $\rho = C(\alpha_1, \alpha_1)$.

Next, we show that there exists a point C' which achieves the sum-rate capacity based on the approach in [36]. To this end, we note that according to this scheme, when transmitter i is in state α_m, it splits its message into two layers denoted by T_{m1}^i and T_{m2}^i with power distribution factors β_m^i and $(1 - \beta_m^i)$, respectively. At the receiver side, the scheme in [36] performs successive decoding with the fixed order specified in Table IV. For the power allocation $\beta_1^1 = \beta_1^2 = 0$ and $\beta_1^1 = \beta_2^2 = 1 - \frac{\alpha_1}{\alpha_2}$, the rates achievable by codebooks $\{T_{m1}^i, T_{m2}^i\}$, for $i, m \in \{1, 2\}$, are given by

$$R_{T_{11}}^1 = 0, \quad R_{T_{11}}^2 = 0, \tag{67}$$

$$R_{T_{12}}^1 = C(\alpha_1, \alpha_1), \quad R_{T_{12}}^2 = C(\alpha_1, 0), \tag{68}$$

$$R_{T_{21}}^1 = C((\alpha_2 - \alpha_1), \alpha_1 + \alpha_2), \quad R_{T_{21}}^2 = C((\alpha_2 - \alpha_1), 2\alpha_1), \tag{69}$$

$$R_{T_{22}}^1 = C(\alpha_1, \alpha_1), \quad R_{T_{22}}^2 = C(\alpha_1, 0). \tag{70}$$

The rates in (67)-(70) are the same as those specified in (60)-(63) when we set $\rho = C(\alpha_1, \alpha_1)$.

Finally, we show that the corner point C' appears strictly on the right side of C. Note that to achievable rate at point D maximizes the average rate of transmitter 1 over all feasible rates allocations for transmitter 2. Therefore, according to Table IV, power allocation according to $\beta_1^1 = 0$, $\beta_1^1 = \beta_2^2 = 1$ and $\beta_1^1 = 1 - \frac{\alpha_1}{\alpha_2}$ is the only such power allocation. The rates achievable by codebooks $\{T_{m1}^i, T_{m2}^i\}$, for $i, m \in \{1, 2\}$, are

$$R_{T_{11}}^1 = 0, \quad R_{T_{11}}^2 = C(\alpha_1, \alpha_1), \tag{71}$$
$$R_{T_{12}}^1 = C(\alpha_1, 0), \quad R_{T_{12}}^2 = 0, \tag{72}$$
$$R_{T_{21}}^1 = C((\alpha_2 - \alpha_1), \alpha_1 + \alpha_2), \quad R_{T_{21}}^2 \leq C(\alpha_1, \alpha_1), \tag{73}$$
$$R_{T_{22}}^1 = C(\alpha_1, \alpha_1), \quad R_{T_{22}}^2 = 0. \tag{74}$$

Hence, (71)- (74) establish that the average achievable rate for transmitter 2 at this point does not fall on line segment CD where the average achievable rates are given by

$$\begin{aligned} &\bar{R}_{T_1} = C(\alpha_1, 0) + q_2 C(\alpha_2 - \alpha_1, \alpha_1 + \alpha_1) = \bar{R}_1, \\ &\bar{R}_{T_2} \leq C(\alpha_1, \alpha_1) < \bar{R}_2. \end{aligned} \tag{75}$$

For any other power allocation such that $\beta_1^2 \neq 1$, we note that the average achievable rate for transmitter 1 is strictly less that that achievable at point D, Hence, for any power allocation for the scheme in [36] achieving the sum-rate capacity falls on line segment CD and strictly to the right of point D.

Appendix C
Corner Points in Figure 3

The coordinates of the corner points of Fig. 3 are specified as follows

$$\begin{aligned} &\mathsf{T} : (0, b_1), \quad \mathsf{U} : (b_2, b_1), \quad \mathsf{V} : (b_7, b_1), \quad \mathsf{W} : (b_3, b_4), \\ &\mathsf{X} : (f_1, f_2), \quad \mathsf{Y} : (b_5, b_6), \quad \mathsf{Z} : (b_5, 0), \end{aligned} \tag{76}$$

where we have defined

$$b_1 \triangleq p_1 C(\alpha_1, 0) + p_2 C(\alpha_2, 0), \tag{77}$$
$$b_2 \triangleq q_1 C(\alpha_1, \alpha_2) + q_2 C(\alpha_2, \alpha_2), \tag{78}$$
$$b_3 \triangleq q_1 \rho_{i^*} + q_2 \hat{\rho}_{j^*}, \tag{79}$$
$$b_4 \triangleq p_1 \mu_{i^*} + p_2 \hat{\mu}_{j^*}, \tag{80}$$
$$b_5 \triangleq q_1 C(\alpha_1, 0) + q_2 C(\alpha_2, 0), \tag{81}$$
$$\begin{aligned} b_6 \triangleq\ & p_{11} C(\alpha_1, \alpha_1) + p_{12} C(\alpha_2, \alpha_1) \\ & + p_{21} C(\alpha_1, \alpha_2) + p_{22} C(\alpha_2, \alpha_2), \end{aligned} \tag{82}$$
$$\begin{aligned} b_7 \triangleq\ & p_{11} C(\alpha_1, \alpha_1) + p_{21} C(\alpha_2, \alpha_1) \\ & + p_{12} C(\alpha_1, \alpha_2) + p_{22} C(\alpha_2, \alpha_2), \end{aligned} \tag{83}$$
$$\begin{aligned} f_1 \triangleq\ & q_1 C(\alpha_1, 0) \\ & + q_2 \left[C\left(\alpha_2 \beta_{12}^1, \alpha_1 + \alpha_2 \beta_{22}^1\right) + C(\alpha_2 \beta_{22}^1, 0) \right], \end{aligned} \tag{84}$$
$$\begin{aligned} f_2 \triangleq\ & p_{11} C(2\alpha_1, 0) \\ & + (p_{12} + p_{21}) C(\alpha_1 + \alpha_2, 0) + p_{22} C(2\alpha_2, 0) - f_1. \end{aligned} \tag{85}$$

and we have defined $i^* \triangleq \arg\max_i \mu_i$ and $j^* \triangleq \arg\max_j \hat{\mu}_j$ for

$$\mu_1 \triangleq p_1 C(\alpha_1, 0) + p_2 [C(\alpha_1 + \alpha_2, 2\alpha_1) + C(\alpha_1, 0)], \tag{86}$$
$$\mu_2 \triangleq p_1 [C(2\alpha_1, \alpha_1 + \alpha_2) + C(\alpha_2, 0)] + p_2 C(\alpha_2, 0), \tag{87}$$
$$\hat{\mu}_1 \triangleq p_1 C(\alpha_1, 0) + p_2 [C(2\alpha_2, \alpha_1 + \alpha_2) + C(\alpha_1, 0)], \tag{88}$$
$$\hat{\mu}_2 \triangleq p_1 [C(\alpha_1 + \alpha_2, 2\alpha_2) + C(\alpha_2, 0)] + p_2 C(\alpha_2, 0), \tag{89}$$
$$\begin{aligned} &\rho_1 \triangleq C(\alpha_1, \alpha_1), \quad \rho_2 \triangleq C(\alpha_1, \alpha_2), \\ &\hat{\rho}_1 \triangleq C(\alpha_2, \alpha_1), \quad \hat{\rho}_2 \triangleq C(\alpha_2, \alpha_2). \end{aligned} \tag{90}$$

Appendix D
Proof of Theorem 3

For characterizing OTUWYZO, we begin by characterizing the corner points of the average capacity region when only one transmitter is active, i.e., corner points T and Z. Then, corner points U and Y, which are achieved when one transmitter is decoded entirely before the other one, are characterized. Finally, we characterize W at which the sum-capacity is achieved. Throughout this section, we denote the rates of transmitter 1 in the *weak* and *strong* channels by R_w^1 and R_s^1, respectively. For transmitter 2, we denote the achievable rates in the four combined states of by $\{R_{ww}^2, R_{ws}^2, R_{sw}^2, R_{ss}^2\}$.

Corner T: By setting $\bar{R}_1 = 0$, $\bar{R}_2$ is bounded by

$$\bar{R}_2 \leq p_1 C(\alpha_1, 0) + p_2 C(\alpha_2, 0) \triangleq b_1. \tag{91}$$

Corner Z: Alternatively, by setting $\bar{R}_2 = 0$, $\bar{R}_1$ is bounded by

$$\bar{R}_1 \leq q_2 C(\alpha_1, 0) + q_2 C(\alpha_2, 0) \triangleq b_5. \tag{92}$$

Corner U: At point U, the message of transmitter 1 is decoded and eliminated before decoding the message of transmitter 2. In each possible combined channel state, the rates of the decodable codebooks transmitted by transmitters 1 and 2 are subject to the following set of inequalities.

Channel state (α_1, α_1):

$$R_w^1 \leq C(\alpha_1, \alpha_1), \quad R_{ww}^2 \leq C(\alpha_1, 0). \tag{93}$$

Channel state (α_1, α_2):

$$R_w^1 \leq C(\alpha_1, \alpha_2), \quad R_{ws}^2 \leq C(\alpha_2, 0). \tag{94}$$

Channel state (α_2, α_1):

$$R_s^1 \leq C(\alpha_2, \alpha_1), \quad R_{sw}^2 \leq C(\alpha_1, 0). \tag{95}$$

Channel state (α_2, α_2):

$$R_s^1 \leq C(\alpha_2, \alpha_2), \quad R_{ss}^2 \leq C(\alpha_2, 0). \tag{96}$$

Hence, the average achievable rates for transmitter 1 and 2 at point U satisfy:

$$\bar{R}_1 \leq q_1 C(\alpha_1, \alpha_2) + q_2 C(\alpha_2, \alpha_2) \triangleq b_2, \tag{97}$$
$$\bar{R}_2 \leq p_1 C(\alpha_1, 0) + p_2 C(\alpha_2, 0) = b_1. \tag{98}$$

Corner Y: At this point, transmitter 2's message is decoded and eliminated first. The outer bounds on the rates of different codebooks are listed below.

Channel state (α_1, α_1):

$$R_{ww}^2 \leq C(\alpha_1, \alpha_1), \quad R_w^1 \leq C(\alpha_1, 0). \tag{99}$$

Channel state (α_1, α_2):

$$R_{ws}^2 \leq C(\alpha_2, \alpha_1), \quad R_w^1; \leq C(\alpha_1, 0). \tag{100}$$

Channel state (α_2, α_1):

$$R_{sw}^2 \le C(\alpha_1, \alpha_2), \quad R_s^1 \le C(\alpha_2, 0). \tag{101}$$

Channel state (α_2, α_2):

$$R_{ss}^2 \le C(\alpha_2, \alpha_2), \quad R_s^1 \le C(\alpha_2, 0). \tag{102}$$

Subsequently, the average achievable rates for transmitters 1 and 2 at point Y are bounded as follows.

$$\bar{R}_1 \le q_1 C(\alpha_1, 0) + q_2 C(\alpha_2, 0) = b_5, \tag{103}$$

$$\bar{R}_2 \le p_{11} C(\alpha_1, \alpha_1) + p_{12} C(\alpha_2, \alpha_1) + p_{21} C(\alpha_1, \alpha_2) + p_{22} C(\alpha_2, \alpha_2) \triangleq b_6. \tag{104}$$

Finally, at point W transmitter 2 adapts its transmission rate such that for any average achievable rate of transmitter 1, the average sum-rate is achieved as follows.

Corner W:

Channel state (α_1, α_1):

$$R_w^1 \le C(\alpha_1, 0), \quad R_{ww}^2 \le C(\alpha_1, 0), \tag{105}$$

$$R_w^1 + R_{ww}^2 \le C(\alpha_1 + \alpha_1, 0). \tag{106}$$

Channel state (α_1, α_2):

$$R_w^1 \le C(\alpha_1, 0), \quad R_{ws}^2 \le C(\alpha_2, 0), \tag{107}$$

$$R_w^1 + R_{ws}^2 \le C(\alpha_1 + \alpha_2, 0). \tag{108}$$

Channel state (α_2, α_1):

$$R_s^1 \le C(\alpha_2, 0), \quad R_{sw}^2 \le C(\alpha_1, 0), \tag{109}$$

$$R_s^1 + R_{sw}^2 \le C(\alpha_1 + \alpha_2, 0). \tag{110}$$

Channel state (α_2, α_2):

$$R_s^1 \le C(\alpha_2, 0), \quad R_{ss}^2 \le C(\alpha_2, 0), \tag{111}$$

$$R_s^1 + R_{ss}^2 \le C(2\alpha_2, 0). \tag{112}$$

In order to find point W we maximize the average rate of transmitter 2 such that the average sum rate capacity is achieved. Consider the following possible four rate allocation for transmitter 2

$$\mu_1 \triangleq p_1 C(\alpha_1, 0) + p_2[C(\alpha_1 + \alpha_2, 2\alpha_1) + C(\alpha_1, 0)], \tag{113}$$

$$\mu_2 \triangleq p_1[C(2\alpha_1, \alpha_1 + \alpha_2) + C(\alpha_2, 0)] + p_2 C(\alpha_2, 0), \tag{114}$$

$$\hat{\mu}_1 \triangleq p_1 C(\alpha_1, 0) + p_2[C(2\alpha_2, \alpha_1 + \alpha_2) + C(\alpha_1, 0)], \tag{115}$$

$$\hat{\mu}_2 \triangleq p_1[C(\alpha_1 + \alpha_2, 2\alpha_2) + C(\alpha_2, 0)] + p_2 C(\alpha_2, 0). \tag{116}$$

where $i^* = \arg\max_i \mu_i$ and $j^* = \arg\max_j \hat{\mu}_j$. For each possible rate allocation in (113)- (116), the corresponding rates of transmitter 1 are identified by

$$\rho_1 \triangleq C(\alpha_1, \alpha_1), \quad \rho_2 \triangleq C(\alpha_1, \alpha_2),$$
$$\hat{\rho}_1 \triangleq C(\alpha_2, \alpha_1), \quad \hat{\rho}_2 \triangleq C(\alpha_2, \alpha_2). \tag{117}$$

Accordingly, the average achievable rates at point W are bounded by

$$\bar{R}_1 \le q_1 \rho_{i^*} + q_2 \hat{\rho}_{j^*} \triangleq b_3, \bar{R}_2 \le p_1 \mu_{i^*} + p_2 \hat{\mu}_{j^*} \triangleq b_4. \tag{118}$$

TABLE V
SUCCESSIVE DECODING SCHEME FOR THEOREM 4

(h_1, h_2)	stage 1	stage 2	stage 3
(α_1, α_1)	W_1^2	U_{11}^1	
(α_1, α_2)	W_2^2	U_{11}^1	
(α_2, α_1)	U_{12}^1	W_3^2	U_{22}^1
(α_2, α_2)	W_4^2	U_{12}^1	U_{22}^1

APPENDIX E
PROOF OF THEOREM 4

We show the region specified by OTUXYZO can be achieved using the layering scheme proposed in Section III-B at transmitter 1. On the other hand, transmitter 2 (who has full CSI) can use four different codebooks each with a rate adapted to a specific combined channel state, denoted by $\{W_1^2, \ldots, W_4^2\}$, with the corresponding rates $\{R_{w_1}^2, \ldots, R_{w_4}^2\}$. Note that irrespective of the layering scheme used at transmitter 1 and 2, the corner points T, U, Y, Z of the average capacity region are achievable as discussed in the proof of Theorem 3 in Appendix D. Hence, we focus on showing the achievability of point X next.

Corner X: The average rates at point X in Fig. 3 can be achieved by implementing the decoding order presented in Table V. In particular, corresponding to each network state, the achievable rates for transmitters 1 and 2 are bounded as follows.

channel state (α_1, α_1):

$$R_{w_1}^2 \le C(\alpha_1, \alpha_1), \quad R_{11}^1 \le C(\alpha_1, 0). \tag{119}$$

Channel state (α_1, α_2):

$$R_{w_2}^2 \le C(\alpha_2, \alpha_1), \quad R_{11}^1 \le C(\alpha_1, 0). \tag{120}$$

Channel state (α_2, α_1):

$$R_{12}^1 \le C\left(\alpha_2 \beta_{12}^1, \alpha_1 + \alpha_2 \beta_{22}^1\right) \triangleq e_1, \tag{121}$$

$$R_{w_3}^2 \le C\left(\alpha_1, \alpha_2 \beta_{22}^1\right) \triangleq e_2, \tag{122}$$

$$R_{22}^1 \le C(\alpha_2 \beta_{22}^1, 0) \triangleq e_3. \tag{123}$$

Channel state (α_2, α_2):

$$R_{w_4}^2 \le C(\alpha_2, \alpha_2) \triangleq e_4, \tag{124}$$

$$R_{12}^1 \le C\left(\alpha_2 \beta_{12}^1, \alpha_2 \beta_{22}^1\right) \triangleq e_5, \tag{125}$$

$$R_{22}^1 \le C(\alpha_2 \beta_{22}^1, 0) \triangleq e_3. \tag{126}$$

By noting that $e_1 \le e_5$, the maximum achievable rate of codebook U_{12}^1 is bounded by e_1. Therefore, setting the rate of codebooks $R_{w_4}^2 = C(\alpha_2 - \alpha_1, \alpha_2 + \alpha_1) + C(\alpha_1, \alpha_2 \beta_{12}^1) < e_1 + e_3$ is feasible since this rate is also less than e_4. The chosen rate of codebook W_4^1 results in average achievable rates at point X that are bounded as follows.

$$\bar{R}_1 \le q_1 C(\alpha_1, 0) + q_2[C\left(\alpha_2 \beta_{12}^1, \alpha_1 + \alpha_2 \beta_{22}^1\right) + C(\alpha_2 \beta_{22}^1, 0)] \triangleq f_1, \tag{127}$$

$$\bar{R}_2 \le p_{11} C(\alpha_1, \alpha_1) + p_{12} C(\alpha_2, \alpha_1) + p_{21} C\left(\alpha_1, \alpha_2 \beta_{22}^1\right)$$

TABLE VI
SUCCESSIVE DECODING ORDER IN THEOREM 5

(h_1, h_2)	stage 1	stage 2	stage 3	stage 4
(α_1, α_1)	U_{11}^2	U_{11}^1		
(α_2, α_1)	U_{12}^1	U_{11}^2	U_{22}^1	
(α_1, α_2)	U_{12}^2	U_{22}^2	U_{11}^1	
(α_2, α_2)	U_{12}^2	U_{12}^1	U_{22}^2	U_{22}^1

$$+ p_{22}[C(\alpha_2 - \alpha_1, \alpha_2 + \alpha_1) + C(\alpha_1, \alpha_2\beta_{12}^1)] \triangleq f_3. \tag{128}$$

Furthermore, the average sum-rate capacity for a MAC channel with full CSIT at both transmitters is

$$\bar{R}_1 + \bar{R}_2 \le p_{11} C\left(2\alpha_1, 0\right) + (p_{12} + p_{21}) C\left(\alpha_1 + \alpha_2, 0\right) + p_{22} C\left(2\alpha_2, 0\right) \triangleq f_4 \tag{129}$$

By noting that $f_3 = f_4 - f_1 = f_2$, equations (127)-(129) show that implementing the decoding order specified in Table V achieves the average sum-rate capacity at point X.

APPENDIX F
PROOF OF THEOREM 5

For this theorem, we show that by adopting the codebook assignment in Section III, the average sum-rate capacity of a two-user MAC with full CSIT is achievable asymptotically under proper power allocation. For this purpose, we find a lower bound on the average sum-rate and show that this lower bound tends to the capacity region with the full CSIT asymptotically. For this purpose, we adopt the fully sequential decoding order specified in Table VI. Clearly, the rate region and the associated average sum-rate yielded by this fully successive decoding approach is a lower bound to the average sum-rate achieved by the decoding approach described in Section III.

Based on the sequential decoding in Table VI, we find the following bounds on the rates of the individual codebooks in different channel combinations.

Channel state (α_1, α_1):

$$R_{11}^2 \le \frac{1}{2}\log\left(1 + \frac{\alpha_1 P_2}{1 + \alpha_1 P_1}\right) \triangleq s_{11}^2, \tag{130}$$

$$R_{11}^1 \le \frac{1}{2}\log\left(1 + \alpha_1 P_1\right) \triangleq s_{11}^1. \tag{131}$$

Channel state (α_2, α_1):

$$R_{12}^1 \le \frac{1}{2}\log\left(1 + \frac{\alpha_2\beta_{12}^1 P_1}{1 + \alpha_2(1-\beta_{12}^1)P_1 + \alpha_1 P_2}\right) \triangleq s_{12}^1, \tag{132}$$

$$R_{11}^2 \le \frac{1}{2}\log\left(1 + \frac{\alpha_1 P_2}{1 + \alpha_2(1-\beta_{12}^1)P_1}\right) \triangleq t_{11}^2, \tag{133}$$

$$R_{22}^1 \le \frac{1}{2}\log\left(1 + \alpha_2(1-\beta_{12}^1)P_1\right) \triangleq s_{22}^1, \tag{134}$$

Channel state (α_1, α_2):

$$R_{12}^2 \le \frac{1}{2}\log\left(1 + \frac{\alpha_2\beta_{12}^2 P_2}{1 + \alpha_1 P_1 + \alpha_2(1-\beta_{12}^2)P_2}\right) \triangleq s_{12}^2, \tag{135}$$

$$R_{22}^2 \le \frac{1}{2}\log\left(1 + \frac{\alpha_2(1-\beta_{12}^2)P_2}{1 + \alpha_1 P_1}\right) \triangleq s_{22}^2, \tag{136}$$

$$R_{11}^1 \le \frac{1}{2}\log\left(1 + \alpha_1 P_1\right) \triangleq t_{11}^1. \tag{137}$$

Channel state (α_2, α_2):

$$R_{12}^2 \le \frac{1}{2}\log\left(1 + \frac{\alpha_2\beta_{12}^2 P_2}{1 + \alpha_2 P_1 + \alpha_2(1-\beta_{12}^2)P_2}\right) \triangleq t_{12}^2, \tag{138}$$

$$R_{12}^1 \le \frac{1}{2}\log\left(1 + \frac{\alpha_2\beta_{12}^1 P_1}{1 + \alpha_2(1-\beta_{12}^1)P_1 + \alpha_2(1-\beta_{12}^2)P_2}\right) \triangleq t_{12}^1, \tag{139}$$

$$R_{22}^2 \le \frac{1}{2}\log\left(1 + \frac{\alpha_2(1-\beta_{12}^2)P_2}{1 + \alpha_2(1-\beta_{12}^1)P_1}\right) \triangleq t_{22}^2, \tag{140}$$

$$R_{22}^1 \le \frac{1}{2}\log\left(1 + \alpha_2(1-\beta_{12}^1)P_1\right) \triangleq t_{22}^1. \tag{141}$$

The bounds in (130)-(141) provide two bounds on the rate of each codebook. Specifically, for each rate R_{jk}^i we have $R_{jk}^i \le \min\{s_{jk}^i, t_{jk}^i\}$. By directly comparing (135) and (138) we find that $s_{12}^2 > t_{12}^2$, since $\alpha_2 > \alpha_1$. For all other five rates it can be readily verified that by setting $\beta_{12}^1 = \beta_{12}^2 = 1 - \frac{\alpha_1}{\alpha_2}$ we obtain $R_{jk}^i = s_{jk}^i = t_{jk}^i$. Hence, by combining the sequential decoding approach and this specific power allocation across codebooks, where both induce sub-optimality, we find the following lower bound, denoted by $R_{\mathrm{s,avg}}$, on the average sum-rate for the proposed broadcast approach.

$$\begin{aligned} 2R_{\mathrm{s,avg}} &= pq(s_{11}^1 + s_{11}^2) + \bar{p}q(s_{12}^1 + s_{11}^2 + s_{22}^1) \\ &\quad + p\bar{q}(t_{12}^2 + s_{22}^2 + s_{11}^1) + \bar{p}\bar{q}(t_{12}^2 + s_{12}^1 + s_{22}^2 + s_{22}^1) \end{aligned} \tag{142}$$

$$\begin{aligned} &= pq\log\left(1 + \alpha_1 P_1 + \alpha_1 P_2\right) \\ &\quad + \bar{p}q\log\left(1 + \alpha_2 P_1 + \alpha_1 P_2\right) \\ &\quad + \bar{p}\bar{q}\log\left(1 + \alpha_2 P_1 + \alpha_2 P_2\right) + p\bar{q}\log\left(1 + \alpha_1 P_1\right) \\ &\quad + p\bar{q}\log\left(1 + \frac{(\alpha_2 - \alpha_1)P_2}{1 + \alpha_2 P_1 + \alpha_1 P_2}\right) \\ &\quad + p\bar{q}\log\left(1 + \frac{\alpha_1 P_2}{1 + \alpha_1 P_1}\right). \end{aligned} \tag{143}$$

On the other hand, the sum-rate capacity with full CSIT at both transmitters, denoted by $C_{\mathrm{s,avg}}$ is given by

$$\begin{aligned} 2C_{\mathrm{s,avg}} &= pq\log\left(1 + \alpha_1 P_1 + \alpha_1 P_2\right) \\ &\quad + p\bar{q}\log\left(1 + \alpha_1 P_1 + \alpha_2 P_2\right) \\ &\quad + \bar{p}q\log\left(1 + \alpha_2 P_1 + \alpha_1 P_2\right) \\ &\quad + \bar{p}\bar{q}\log\left(1 + \alpha_2 P_1 + \alpha_2 P_2\right). \end{aligned} \tag{144}$$

Finally, let $d(p, q)$ denote the difference between the lower and upper bounds on the average sum-rate provided by (143) and (144), respectively. Hence,

$$\begin{aligned} d(p,q) &= C_{\mathrm{s,avg}} - R_{\mathrm{s,avg}} \\ &= \frac{p\bar{q}}{2}\log\left(\frac{(1 + \alpha_1 P_1 + \alpha_2 P_2)(1 + \alpha_2 P_1 + \alpha_1 P_2)}{(1 + \alpha_2 P_1 + \alpha_2 P_2)(1 + \alpha_1 P_1 + \alpha_1 P_2)}\right). \end{aligned} \tag{145}$$

By examining (145), it can be verified that the term $d(p,q)$ is maximized at $p=1$ and $q=0$, rendering

$$d_{\max} \triangleq \max_{p,q} d(p,q) = \frac{1}{2}\left[\log\left(\frac{(1+\alpha_1P_1+\alpha_2P_2)(1+\alpha_2P_1+\alpha_1P_2)}{(1+\alpha_2P_1+\alpha_2P_2)(1+\alpha_1P_1+\alpha_1P_2)}\right)\right]. \quad (146)$$

In the low power regime, we show that when either P_1 or P_2 approach 0, the term $d_{\max}$ also approaches 0 faster than $R_{\mathrm{s,avg}}$ given in (143), and also faster than $C_{\mathrm{s,avg}}$ given in (144). First, we consider the case when $P_1 \to 0$ while P_2 is constant. It can be readily verified from (143), (144), and (146) that $C_{\mathrm{s,avg}}$ is equal to $R_{\mathrm{s,avg}}$, where both approach a finite non-zero value while $d_{\max}$ approaches 0. Specifically, we have

$$\lim_{P_1\to 0}\frac{d_{\max}}{R_{\mathrm{s,avg}}} = \frac{0}{\log(1+\alpha_2P_2)} = 0. \quad (147)$$

A similar behavior can be verified for the case that P_2 approaches 0 and P_1 remains fixed. Secondly, for the case where both P_1 and P_2 approach 0 at different rates, i.e., $P_1 \to 0$, $P_2 \to 0$, by applying l'Hôpital's rule for multi-variable functions [40] we have

$$\lim_{\substack{P_1\to 0,P_2\to 0\\ P_1\neq P_2}}\frac{d_{\max}}{R_{\mathrm{s,avg}}} = \frac{\frac{\partial d_{\max}}{\partial P_1}}{\frac{\partial R_{\mathrm{s,avg}}}{\partial P_1}} = \frac{0}{\alpha_1} = 0, \quad (148)$$

and

$$\lim_{\substack{P_1\to 0,P_2\to 0\\ P_1\neq P_2}}\frac{d_{\max}}{R_{\mathrm{s,avg}}} = \frac{\frac{\partial d_{\max}}{\partial P_1}}{\frac{\partial C^{\mathrm{full}}_{\mathrm{s,avg}}}{\partial P_1}} = \frac{0}{\alpha_1} = 0. \quad (149)$$

Finally, for the case of equal transmission power at both transmitters, i.e., $P_1 = P_2 = P$ we have

$$R_{\mathrm{s,avg}} = \frac{1}{2}\log\left(\frac{(1+2\alpha_2P)(1+2\alpha_1P)}{(1+(\alpha_1+\alpha_2)P)}\right), \quad (150)$$

$$C_{\mathrm{s,avg}} = \frac{1}{2}\log(1+(\alpha_1+\alpha_2)P), \quad (151)$$

$$d_{\max} = \frac{1}{2}\left[\log\left(\frac{(1+(\alpha_1+\alpha_2)P)^2}{(1+2\alpha_2P)(1+2\alpha_1P)}\right)\right]. \quad (152)$$

Hence, when $P \to 0$, it can be readily verified from (150)-(152) that $d_{\max}, R_{\mathrm{s,avg}}$ and $C_{\mathrm{s,avg}}$ approach 0. Hence, by applying l'Hôpital's rule we have

$$\lim_{P\to 0}\frac{d_{\max}}{R_{\mathrm{s,avg}}} = \frac{2(\alpha_1+\alpha_2)-2(\alpha_1+\alpha_2)}{2\alpha_2} = 0, \quad (153)$$

and

$$\lim_{P\to 0}\frac{d_{\max}}{C_{\mathrm{s,avg}}} = \frac{2(\alpha_1+\alpha_2)-2(\alpha_1+\alpha_2)}{\alpha_1+\alpha_2} = 0. \quad (154)$$

As a result, from (147), (153), and (154) we conclude that the sum-rate capacity is achieved for the proposed broadcast strategy for sufficiently small transmission power at either one of the transmitters or at both transmitters simultaneously. Additionally, in the high power regime, if either P_1 or P_2 approach infinity, then $d_{\max} \to 0$ indicating that the sum-rate capacity is achieved in the asymptote of high power.

APPENDIX G
CONSTANTS OF THEOREM 6

$$b_1(j,m) \triangleq C(\alpha_j\beta^1_{jj}, \alpha_m B_2(j,m)), \quad \forall j\in\{1,\dots,\ell\}, m\in\{j,\dots,\ell\}, \quad (155)$$

$$b_2(j,i) \triangleq C(\alpha_j\beta^2_{jj}, \alpha_m B_1(j,m)), \quad \forall j\in\{1,\dots,\ell\}, \quad (156)$$

$$b_3(j,n,m) \triangleq C(\alpha_n\beta^1_{jn}, \alpha_n B_1(j,n)+\alpha_j B_2(j,j)), \quad \forall n\in\{j+1,\dots,\ell\}, m\in\{j,\dots,\ell\}, \quad (157)$$

$$b_4(j,n,m) \triangleq C(\alpha_n\beta^2_{jn}, \alpha_j B_1(j,m)+\alpha_n B_2(j,n)), \quad \forall n\in\{j+1,\dots,\ell\}, \quad (158)$$

$$b_5(m) \triangleq C(\alpha_m\beta^1_{mm}+\alpha_n\beta^2_{mm}), \quad \forall m\in\{1,\dots,\ell\}, \quad (159)$$

$$b_6(m,n) \triangleq C(\alpha_m\beta^1_{mm}+\alpha_n\beta^2_{mn}, \alpha_n B_2(m,n)), \quad \forall m<n, \forall n\in\{m+1,\dots,\ell\}, \quad (160)$$

$$b_7(m,n) \triangleq C(\alpha_n\beta^1_{mn}+\alpha_m\beta^2_{mm}, \alpha_n B_1(m,n)), \quad \forall m<n, \forall n\in\{m+1,\dots,\ell\}, \quad (161)$$

$$b_8(k,m,n) \triangleq C\left(\alpha_m\beta^1_{km}+\alpha_n\beta^2_{kn}, \alpha_m B_1(k,m)+\alpha_n B_2(k,n)\right), \quad \forall k<m, \forall n\in\{m,\dots,\ell\}, \quad (162)$$

$$b_9(k,m,n) \triangleq C\left(\alpha_n\beta^1_{kn}+\alpha_m\beta^2_{km}, \alpha_n B_1(k,n)+\alpha_m B_2(k,m)\right), \quad \forall k<m, \forall n\in\{m,\dots,\ell\}, \quad (163)$$

$$r_1(n,m) \triangleq \min_m\{\sum_{j=1}^{\ell} b_1(j,m)+b_3(j,n,m)\}, \quad (164)$$

$$r_2(n,m) \triangleq \min_m\{\sum_{j=1}^{\ell} b_2(j,m)+b_4(j,n,m), \quad (165)$$

$$r_3(n,m) \triangleq \sum_{\forall k<m} b_5(m)+b_7(m,n)+b_9(k,m,n), \quad (166)$$

$$r_4(n,m) \triangleq \sum_{\forall k<m} b_5(m)+b_6(m,n)+b_8(k,m,n). \quad (167)$$

where $B_1(m,n) \triangleq 1-\sum_{i=1}^{m}\beta^1_{in}$ and $B_2(m,n) \triangleq 1-\sum_{i=1}^{m}\beta^2_{in}$, $\forall m<n$ and $n\in\{m+1,\dots,\ell\}$.

REFERENCES

[1] E. Biglieri, J. Proakis, and S. Shamai, "Fading channels: Information-theoretic and communications aspects," *IEEE Trans. Inf. Theory*, vol. 44, no. 6, pp. 2619–2692, Oct. 1998.

[2] L. H. Ozarow, S. Shamai, and A. D. Wyner, "Information theoretic considerations for cellular mobile radio," *IEEE Trans. Veh. Technol.*, vol. 43, no. 2, pp. 359–378, May 1994.

[3] S. V. Hanly and D. N. C. Tse, "Multiaccess fading channel—Part II: Delay limited capacity," *IEEE Trans. Inf. Theory*, vol. 44, no. 7, pp. 2816–2831, Nov. 1998.

[4] L. Li, N. Jindal, and A. Goldsmith, "Outage capacities and optimal power allocation for fading multiple-access channels," *IEEE Trans. Inf. Theory*, vol. 51, no. 4, pp. 1326–1347, Apr. 2005.

[5] R. Narasimhan, "Individual outage rate regions for fading multiple access channels," in *Proc. IEEE Int. Symp. Inf. Theory*, Nice, France, Jun. 2007, pp. 1571–1575.

[6] A. Haghi, R. Khosravi-Farsani, M. R. Aref, and F. Marvasti, "The capacity region of fading multiple access channels with cooperative encoders and partial CSIT," in *Proc. IEEE Int. Symp. Inf. Theory*, Austin, TX, USA, Jun. 2010, pp. 485–489.

[7] A. Das and P. Narayan, "Capacities of time-varying multiple-access channels with side information," *IEEE Trans. Inf. Theory*, vol. 48, no. 1, pp. 4–25, Jan. 2001.

[8] S. Jafar, "Capacity with causal and noncausal side information: A unified view," *IEEE Trans. Inf. Theory*, vol. 52, no. 12, pp. 5468–5474, Dec. 2006.

[9] T. Cover, "Broadcast channels," *IEEE Trans. Inf. Theory*, vol. IT-18, no. 1, pp. 2–14, Jan. 1972.

[10] S. Shamai, "A broadcast strategy for the Gaussian slowly fading channel," in *Proc. IEEE Int. Symp. Inf. Theory*, Ulm, Germany, Jun./Jul. 1997, p. 150.

[11] S. Verdú and S. Shamai, "Variable-rate channel capacity," *IEEE Trans. Inf. Theory*, vol. 56, no. 6, pp. 2651–2667, Jun. 2010.

[12] T. T. Kim and M. Skoglund, "On the expected rate of slowly fading channels with quantized side information," *IEEE Trans. Commun.*, vol. 55, no. 4, pp. 820–829, Apr. 2007.

[13] R. Ahlswede, "Multi-way communication channels," in *Proc. IEEE Int. Symp. Inf. Theory*, Hong Kong, Jun. 1971, pp. 103–105.

[14] H. Liao, "Multiple access channels," Ph.D. dissertation, Dept. Elec. Eng., Univ. Hawaii, Honolulu, HI, USA, 1972.

[15] Y. Cemal and Y. Steinberg, "The multiple-access channel with partial state information at the encoders," *IEEE Trans. Inf. Theory*, vol. 51, no. 11, pp. 3992–4003, Nov. 2005.

[16] G. Como and S. Yüksel, "On the capacity of memoryless finite-state multiple-access channels with asymmetric state information at the encoders," *IEEE Trans. Inf. Theory*, vol. 57, no. 3, pp. 1267–1273, Mar. 2011.

[17] U. Basher, A. Shirazi, and H. H. Permuter, "Capacity region of finite state multiple-access channels with delayed state information at the transmitters," *IEEE Trans. Inf. Theory*, vol. 58, no. 6, pp. 3430–3452, Jun. 2012.

[18] N. Şen, F. Alajaji, S. Yüksel, and G. Como, "Multiple access channel with various degrees of asymmetric state information," in *Proc. IEEE Int. Symp. Inf. Theory*, Cambridge, MA, USA, Jul. 2012, pp. 1697–1701.

[19] N. Şen, F. Alajaji, S. Yüksel, and G. Como, "Memoryless multiple access channel with asymmetric noisy state information at the encoders," *IEEE Trans. Inf. Theory*, vol. 59, no. 11, pp. 7052–7070, Nov. 2013.

[20] A. Lapidoth and Y. Steinberg, "The multiple-access channel with causal side information: Double state," *IEEE Trans. Inf. Theory*, vol. 59, no. 3, pp. 1379–1393, Mar. 2013.

[21] A. Lapidoth and Y. Steinberg, "The multiple-access channel with causal side information: Common state," *IEEE Trans. Inf. Theory*, vol. 59, no. 1, pp. 32–50, Jan. 2013.

[22] M. Li, O. Simeone, and A. Yener, "Multiple access channels with states causally known at transmitters," *IEEE Trans. Inf. Theory*, vol. 59, no. 3, pp. 1394–1404, Mar. 2013.

[23] S. P. Kotagiri and J. N. Laneman, "Multiaccess channels with state known to some encoders and independent messages," *EURASIP J. Wireless Commun. Netw.*, vol. 2008, no. 1, p. 450680, Mar. 2008.

[24] A. Lapidoth and Y. Steinberg, "The multiple access channel with two independent states each known causally to one encoder," in *Proc. IEEE Int. Symp. Inf. Theory*, Austin, TX, USA, Jun. 2010, pp. 480–484.

[25] H. H. Permuter, S. Shamai, and A. Somekh-Baruch, "Message and state cooperation in multiple access channels," *IEEE Trans. Inf. Theory*, vol. 57, no. 10, pp. 6379–6396, Oct. 2011.

[26] I. H. Wang, "Approximate capacity of the dirty multiple-access channel with partial state information at the encoders," *IEEE Trans. Inf. Theory*, vol. 58, no. 5, pp. 2781–2787, May 2012.

[27] M. J. Emadi, M. N. Khormuji, M. Skoglund, and M. R. Aref, "Multilayer Gelfand–Pinsker strategies for the generalised multiple-access channel," *IET Commun.*, vol. 8, no. 8, pp. 1296–1308, May 2014.

[28] M. Monemizadeh, E. Bahmani, G. A. Hodtani, and S. A. Seyedin, "Gaussian doubly dirty compound multiple-access channel with partial side information at the transmitters," *IET Commun.*, vol. 8, no. 12, pp. 2181–2192, Aug. 2014.

[29] S. Sreekumar, B. K. Dey, and S. R. B. Pillai, "Distributed rate adaptation and power control in fading multiple access channels," *IEEE Trans. Inf. Theory*, vol. 61, no. 10, pp. 5504–5524, Oct. 2015.

[30] M. J. Emadi, M. Zamanighomi, and M. R. Aref, "Multiple-access channel with correlated states and cooperating encoders," *IET Commun.*, vol. 6, no. 13, pp. 1857–1867, Sep. 2012.

[31] H. H. Permuter, T. Weissman, and J. Chen, "Capacity region of the finite-state multiple-access channel with and without feedback," *IEEE Trans. Inf. Theory*, vol. 55, no. 6, pp. 2455–2477, Jun. 2009.

[32] S. Shamai, "A broadcast approach for the multiple-access slow fading channel," in *Proc. IEEE Int. Symp. Inf. Theory*, Sorrento, Italy, Jun. 2000, p. 128.

[33] P. Minero and D. N. C. Tse, "A broadcast approach to multiple access with random states," in *Proc. IEEE Int. Symp. Inf. Theory*, Nice, France, Jun. 2007, pp. 2566–2570.

[34] S. Kazemi and A. Tajer, "A broadcast approach to multiple access adapted to the multiuser channel," in *Proc. IEEE Int. Symp. Inf. Theory*, Aachen, Germany, Jun. 2017, pp. 883–887.

[35] S. Kazemi and A. Tajer, "Multiaccess communication via a broadcast approach adapted to the multiuser channel," *IEEE Trans. Commun.*, vol. 66, no. 8, pp. 3341–3353, Aug. 2018.

[36] S. Zou, Y. Liang, and S. S. Shitz, "Multiple access channel with state uncertainty at transmitters," in *Proc. IEEE Int. Symp. Inf. Theory*, Istanbul, Turkey, Jul. 2013, pp. 1466–1470.

[37] P. Minero, M. Franceschett, and D. N. C. Tse, "Random access: An information-theoretic perspective," *IEEE Trans. Inf. Theory*, vol. 58, no. 2, pp. 909–930, Feb. 2012.

[38] R. Knopp and P. A. Humblet, "Information capacity and power control in single-cell multiuser communications," in *Proc. IEEE International Conference on Communications*, Seattle, WA, USA, vol. 1, Jun. 1995, pp. 331–335.

[39] A. El Gamal and Y.-H. Kim, *Network Information Theory*. Cambridge, U.K.: Cambridge Univ. Press, 2011.

[40] G. R. Lawlor, "A L'hospital's rule for multivariable functions," Aug. 2012, *arXiv:1209.0363*. [Online]. Available: https://arxiv.org/abs/1209.0363